Glacial geomorphology of the central Barents Sea Implications for the dynamic deglaciation of the Barents Sea Ice Sheet

Newton, A. M. W., & Huuse, M. (2017). Glacial geomorphology of the central Barents Sea Implications for the dynamic deglaciation of the Barents Sea Ice Sheet. *Marine Geology*, *387*, 114-131. https://doi.org/10.1016/j.margeo.2017.04.001

Published in:
Marine Geology

Document Version:
Publisher's PDF, also known as Version of record

Marine Geology 387 (2017) 114–131

Contents lists available at ScienceDirect

Marine Geology

journal homepage: www.elsevier.com/locate/margo

Glacial geomorphology of the central Barents Sea: Implications for the dynamic deglaciation of the Barents Sea Ice Sheet

Andrew M.W. Newton*, Mads Huuse

School of Earth and Environmental Sciences, University of Manchester, M13 9PL, UK
Cryosphere Research at Manchester, University of Manchester, M13 9PL, UK

ARTICLE INFO

Keywords:
Barents Sea
Glacial geomorphology
Last Glacial Maximum
Ice stream
Deglaciation
Palaeo-glaciology
Bathymetry

ABSTRACT

Contemporary climate change has resulted in great uncertainty in how glaciers and ice sheets around the Earth might evolve. It has long been appreciated that the contemporary West Antarctic Ice Sheet (WAIS) shares many similarities with the former Barents Sea Ice Sheet (BSIS). Therefore, an increasing number of studies have sought to investigate the Barents Sea glacial record to better understand marine-based glaciation. This paper reports the analysis of a new high-resolution bathymetric survey covering ~55,000 km^2 in the central Barents Sea. The relative chronologies of newly-mapped glacial landforms such as mega-scale glacial lineations, grounding-zone wedges, moraines, and crevasse-squeeze ridges are used to reconstruct the ice sheet dynamics in the central Barents Sea. Our results show that the ice sheet responded dynamically with different periods of retreat, advance, and stagnation observed. These new landform records have been integrated with other geomorphological records in order to reconstruct the retreat pattern of the BSIS between 17–14 ka, when the Fennoscandian Ice Sheet is thought to have uncoupled from the BSIS. Our data shows that the dynamic drawdown of the ice sheet saddle by ice streams was probably the primary mechanism in separating the two ice sheets. After the ice sheets uncoupled, the BSIS is shown to have retreated episodically with several periods of relative stability. Geomorphological records such as those from the BSIS can be used to constrain ice sheet modelling and will help to develop a clearer understanding of marine-based glaciation and the role of ice streams in driving ice sheet evolution.

1. Introduction

Sedimentary records on high-latitude margins are important for reconstructing palaeo-ice sheets and their dynamics (Solheim et al., 1990; Jansen and Sjøholm, 1991; Vorren and Laberg, 1997; Ottesen et al., 2005). Mercer (1970) first suggested that an ice sheet similar in size to the West Antarctic Ice Sheet (WAIS) may have existed over the Barents Sea shelf at the Last Glacial Maximum (LGM). Subsequently, investigating the offshore stratigraphy and geomorphology of the Barents Sea has become an important area of research because the former Barents Sea Ice Sheet (BSIS) has been suggested as a possible analogue for understanding contemporary change on the WAIS (Andreassen and Winsborrow, 2009).

On a reverse slope, an initial perturbation of the grounding-line location (the area where ice becomes sufficiently buoyant to float) can lead to increased ice sheet discharge (Weertman, 1974; Hughes, 1981; Schoof, 2007) until a new steady-state is reached (Joughin and Alley, 2011; Jakobsson et al., 2012a; Jamieson et al., 2012). This scenario is concerning because of the potential sea level contribution of the WAIS (Rohling et al., 2009) and ongoing observations of grounding-line retreat and ice stream thinning and velocity increase (Pritchard et al., 2009; Wingham et al., 2009; Rignot et al., 2011). Since the LGM the WAIS has retreated up to 1000 km (Bentley et al., 2014) and the BSIS has disappeared. Although the geological setting of the WAIS is different to that of the BSIS, understanding the retreat of different marine-based ice sheets will allow for a more complete model of marine-based glaciation to be developed (Denton et al., 2010; Ingólfsson and Landvik, 2013).

This paper presents analysis of high-resolution bathymetric data in the central Barents Sea (Fig. 1a). The ice sheet history in the central Barents Sea is poorly understood due to limited data availability (Polyak et al., 1995; Bjarnadóttir et al., 2014). Geomorphological and geochronological compilations have suggested that the BSIS and the Fennoscandian Ice Sheet (FIS) separated in the central Barents Sea between 16–15 ka (Hughes et al., 2016; Stroeven et al., 2016) (Fig. 1b, c) and the aim of this study was to provide new insight into how that uncoupling process evolved. This was achieved by carrying out a geomorphological analysis of the seafloor and mapping landform assemblages preserved from the last glacial cycle.

* Corresponding author.
E-mail address: amwnewton@gmail.com (A.M.W. Newton).

http://dx.doi.org/10.1016/j.margeo.2017.04.001
Received 17 October 2016; Received in revised form 31 March 2017; Accepted 5 April 2017
Available online 07 April 2017

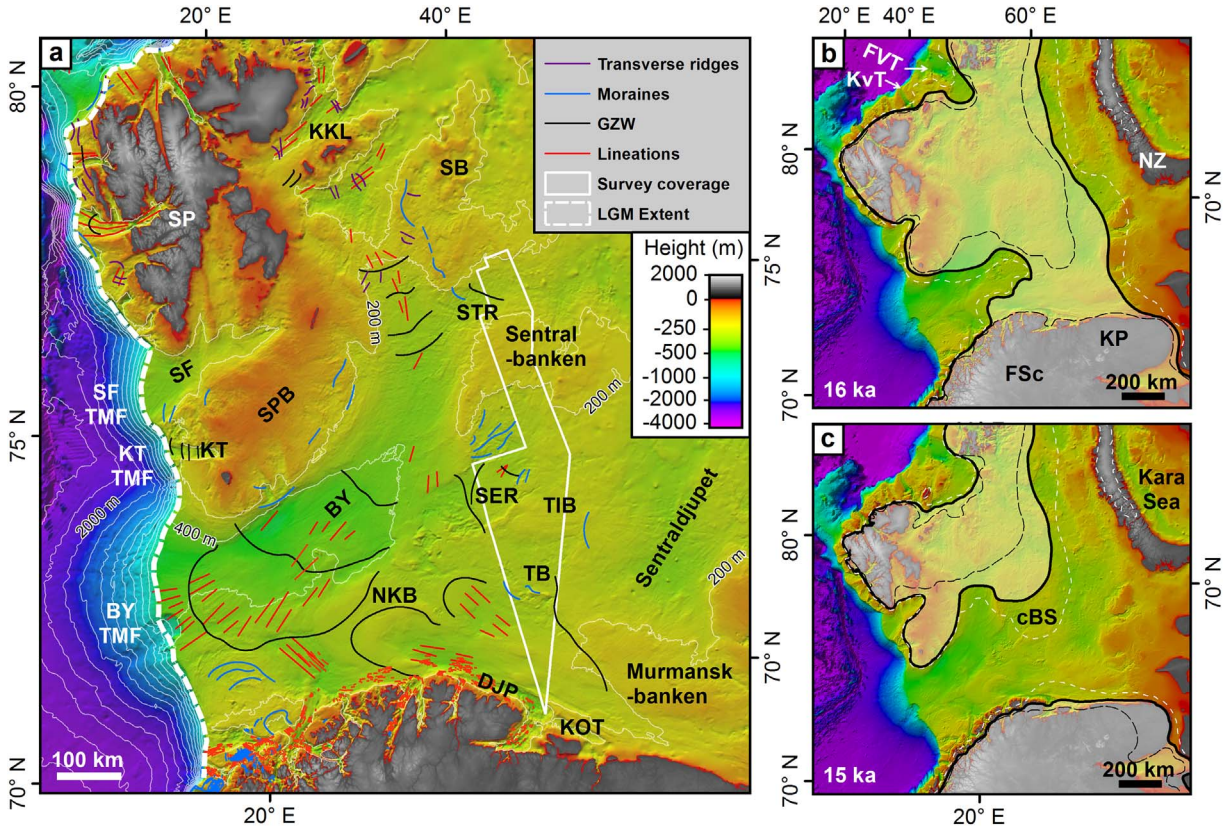

Fig. 1. a) Barents Sea regional bathymetry and hinterland topography from the International Bathymetric Chart of the Arctic Ocean v.3.0 (IBCAO) (Jakobsson et al., 2012b). Contours are every 200 m and the seafloor geomorphology is collated from a number of studies (Ottesen et al., 2008b; Winsborrow et al., 2010; Bjarnadóttir et al., 2014; Jakobsson et al., 2014). The data used in this study is shown with the white outline; b-c) time-slice reconstructions of the Barents Sea Ice Sheet at 16 ka and 15 ka from Hughes et al. (2016). It is important to note that the spatio-temporal evolution of the margin here is uncertain and the white and black dashed lines are the maximum and minimum reconstructions, respectively. The semi-transparent polygons with the thick black outline represents the 'most-credible' reconstruction from Hughes et al. (2016) and it is these reconstructions we use to aid our own. Key place names and abbreviations are as follows: Bjørnøyrenna (BY), central Barents Sea (cBS), Djuprenna (DJP), Fennoscandia (FSc), Franz Victoria Trough (FVT), Grounding-zone Wedge (GZW), Kola Peninsula (KP), Kong Karls Lands (KKL), Kola Trough (KOT), Kveithola Trough (KT), Kvitøya Trough (KvT), Nordkappbanken (NKB), Novaya Zemlya (NZ), Sentralbankrenna (SER), Spitsbergen (SP), Spitsbergenbanken (SPB), Storbanken (SB), Storbankrenna (STR), Storfjordrenna (SF), Thor Iversen-banken (TIB), Tiddlybanken (TB), and Trough Mouth Fan (TMF). Map projection here and in all subsequent figures is ED50 UTM Zone 33.

2. Study area

2.1. Geological history

The Barents Sea, from 70–79°N and 14–58°E, is one of the world's widest continental shelves (Andreassen and Winsborrow, 2009) (Fig. 1a). The northern and western margins were formed during Cenozoic rifting of the North Atlantic at ~55–54 Ma (Faleide et al., 1993, 1996; Gernigon et al., 2014). Subsidence since the Early Cretaceous has led to the accumulation of a major Cretaceous deposit composed of shale and claystone (Gabrielsen et al., 1990; Faleide et al., 2010). The Cenozoic succession consists of deep-marine sediment in the early Paleocene and shallow-marine in the Oligo-Miocene (Ryseth et al., 2003), before the dominance of glacial facies through the Plio-Pleistocene (Butt et al., 2000; Knies et al., 2009; Laberg et al., 2011).

The shelf is characterised by shallow banks of 100–200 m water depth, that are separated by cross-shelf troughs 300–500 m deep that extend to the shelf edge (Fig. 1a). The most prominent trough, Bjørnøyrenna, is ~700–800 km long, 100–200 km wide, and has been excavated by glacial erosion since ~1.5 Ma (Elverhøi and Solheim, 1983; Laberg et al., 2011). The sedimentary cover in the Barents Sea is composed of glacial sediments deposited on top of the Upper Regional Unconformity and typically measures less than ~100 m thick, with the exception of the trough mouth fans (TMFs) and the bank areas (Solheim and Kristoffersen, 1984; Faleide et al., 1996; Solheim et al., 1996).

2.2. Glacial history

Since 3.5 Ma the Barents Sea has experienced multiple glaciations with more extensive glaciation occurring after ~1.5 Ma and further intensification after ~1.0 Ma (Vorren et al., 1988; Knies et al., 2009). TMFs on the western margin of the Barents Sea record multiple shelf-wide glaciations throughout this period (Vorren and Laberg, 1997). The large size of the Bjørnøya TMF, with a volume of ~340,000 km^3 (Fiedler and Faleide, 1996), reflects the frequent reoccupation of Bjørnøyrenna by ice streams during the Plio-Pleistocene (Vorren and Laberg, 1997). Ice streams are narrow, linear zones of fast-flowing ice where the ice sheet velocity is significantly greater than the surrounding ice (Bennett, 2003). Palaeo-ice streams can be identified through the observations of landforms such as mega-scale glacial lineations (MSGLs) (Stokes and Clark, 1999).

The BSIS reached the shelf edge during the LGM between 21.5–18.1 cal. ka BP (Fig. 2) and also at some time prior to 26.5 cal. ka BP during the late Weichselian (Laberg and Vorren, 1996). The Bjørnøyrenna Ice Stream was the main drainage outlet of the ice sheet during the LGM and it is thought that its retreat from the outer shelf started by 18–16 cal. ka BP (Rasmussen et al., 2007; Jessen et al., 2010; Junttila et al., 2010; Rüther et al., 2012). Observations of grounding-zone wedges, crevasse-squeeze ridges, moraines, and MSGLs suggest that retreat of the ice stream through the Bjørnøyrenna trough was interrupted by stillstands and readvances related to changes in backstresses, ice sheet velocity, and ice sheet thinning (Winsborrow et al.,

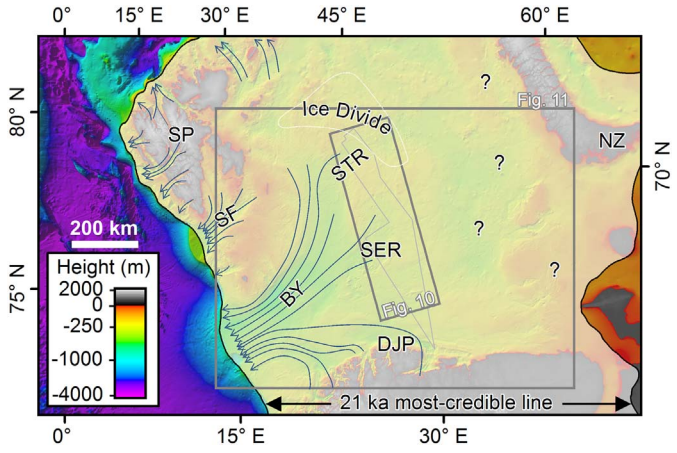

Fig. 2. Extent of the Barents Sea Ice Sheet at the LGM. At this time the Eurasian Ice Sheet covered its maximum total area and does not reflect the maximum extent of the different margins around the ice sheet. The ice sheet margin is the 21 ka 'most-credible' reconstruction from Hughes et al. (2016). Blue arrows show fast-flowing ice from Ottesen et al. (2005). It is important to note that it is not currently known with certainty when the individual ice streams were operating. The eastern margin of the BSIS is particularly uncertain due to the lack of available data. Abbreviations the same as Fig. 1. The geographical extents of Figs. 10 and 11 are indicated as is the outline of the survey. (For interpretation of the references to colour in this figure legend, the reader is referred to the web version of this article.)

2010; Rüther et al., 2011; Andreassen et al., 2014; Bjarnadóttir et al., 2014). As the Bjørnøyrenna Ice Stream retreated through the trough, ice divides migrated in response to the changing ice sheet topography (Bjarnadóttir et al., 2014; Piasecka et al., 2016). The Kveithola and Kong Karls Land areas were completely deglaciated by about 11.2 cal. ka BP (Bondevik et al., 1995; Wohlfarth et al., 1995).

A limited amount of high-resolution data from the central Barents Sea has shown the location of the ice margin on Thor Iversen-banken and Murmanskbanken shortly before deglaciation occurred between 15.6–14.2 cal. ka BP (Polyak et al., 1995; Svendsen et al., 2004; Bjarnadóttir et al., 2014). The deglaciation chronology for the central Barents Sea is not only hampered by the lack of dating control, but also by the lack of extensive high-resolution geophysical and geological data.

3. Data and methods

Bathymetry for the central Barents Sea was provided from the MAREANO multibeam data set (available at www.mareano.no) collected by the Norwegian Hydrographic Service (Fig. 3). The survey is 55,000 km^2 and has a 5 m horizontal resolution. Landforms were then interpreted and mapped in ArcGIS and Petrel. Glacial inversion techniques assert that the creation, modification, and preservation of glacial landforms are determined by the thermal conditions at the ice sheet base and ice sheet dynamics (Kleman and Borgström, 1996; Kleman et al., 2006). This model allows geomorphologists to make the distinction between areas of fast- and slow-flowing ice. For warm-based ice the base of the ice sheet is at the pressure melting point, causing deposition and erosion rates to be several orders of magnitude higher than for cold-based ice (Kleman et al., 2006). The superposition of landforms can also be used to indicate the relative chronology of different landforms (Clark, 1993, 1997).

Using previous examples of glacial landforms (e.g. Dowdeswell et al., 2016), features were documented and mapped across the survey (Figs. 4–8). Landforms from other publications in the Barents Sea (e.g. Svendsen et al., 2004; Andreassen and Winsborrow, 2009; Winsborrow et al., 2010; Bjarnadóttir et al., 2013, 2014; Andreassen et al., 2014; Piasecka et al., 2016) were also digitised to create a regional geomorphological record. The combined landform records in the central Barents Sea were generalised into flow-sets where each flow-set demonstrated a spatial and geometric coherency, or a relationship with other landforms that could be explained by glacial processes known to occur on contemporary ice sheets (Fig. 9) (Kleman and Borgström, 1996; Clark, 1997).

The retreat of the ice sheet is then presented as a number of time-slices at a local (Fig. 10) and regional level (Fig. 11) between 17–14 ka, when the BSIS and FIS are thought to have separated (Hughes et al., 2016; Stroeven et al., 2016). Using the 'most-credible' time-slices from Hughes et al. (2016) before and after separation, several intermittent time-slices were reconstructed showing how the ice sheets uncoupled. This involved the use of cross-cutting flow-sets and judicious use of seafloor topography to intuitively develop plausible patterns of ice sheet flow that complemented landform records (i.e. through a trough, or convergence of ice to aid ice streaming). Without a network of dating constraints we assume coevality between different landform observations (i.e. stillstands in Bjørnøyrenna are coeval with stillstands in Sentralbankrenna) to carefully develop a realistic reconstruction. In areas where landform records are lacking, the ice margin is reconstructed with successively smaller margins between known ice margins. Although this is a simplification, it is the most plausible way of reconstructing the pattern of retreat, as long as correlations are carefully considered and the reconstruction is the simplest possible.

In the regional reconstruction (Fig. 11), observed readvances (e.g. Bjarnadóttir et al., 2014) during the retreat of the ice margin are not documented. This allows for a general geographic pattern of retreat to be developed. Similar methods and workflows are common and have been used to reconstruct several palaeo-ice sheets (Boulton and Clark, 1990; Clark, 1993, 1997; Kleman and Borgström, 1996; Kleman et al., 2006; Greenwood and Clark, 2009; Winsborrow et al., 2011; Clark et al., 2012; Hughes et al., 2014). The caveat to such an approach is that neighbouring ice streams in northern Norway have shown different rates and styles of retreat after the LGM (Stokes et al., 2014). However, given that the objective is to provide a regional pattern of retreat and separation of the BSIS from the FIS, such an approach is reasonable.

4. Results: description and interpretation of submarine landforms

In the survey investigated here, a number of banks and troughs are partially imaged in the multibeam data (Fig. 3). These include the Storbankrenna and Sentralbankrenna troughs with water depths varying from ~280–355 m. The troughs are separated by Sentralbanken, Thor Iversen-banken, and Tiddlybanken where water depths decrease to 140–280 m (Fig. 3). Mapping of the survey revealed an extensive suite of landforms that are described and interpreted below.

4.1. Streamlined bedforms

Streamlined bedforms are present across Storbankrenna (Figs. 4a–c), Sentralbankrenna (Fig. 4d), and in the low topography area north of Tiddlybanken (Fig. 4e). In Storbankrenna and Sentralbankrenna the features appear to continue outside of the survey. These features show a parallel conformity and are generally 3–16 km long, 100–600 m wide, and 5–10 m high. These features share morphological similarities to mega-scale glacial lineations (MSGLs) formed beneath areas of fast-flowing ice and are indicative of ice streaming or surging (Clark, 1993; Stokes and Clark, 1999, 2001; Ottesen et al., 2008a; Spagnolo et al., 2014). MSGLs form-parallel to ice flow and, although the formation of MSGLs is debated, it is generally thought to relate to streamlining or deformation of weak, saturated tills (Clark et al., 2003).

The northern MSGLs suggest NNE-SSW ice sheet flow (Fig. 4a, b) and the reworking of a ridge feature that is interpreted as a moraine (see Section 4.4) implies advance of the ice margin (Fig. 4a). These MSGLs appear to continue onto the southern flank of Sentralbankrenna where they have been significantly reworked by iceberg scouring (see Section 4.8) (Fig. 4b). In Storbankrenna a number of subtle MSGLs

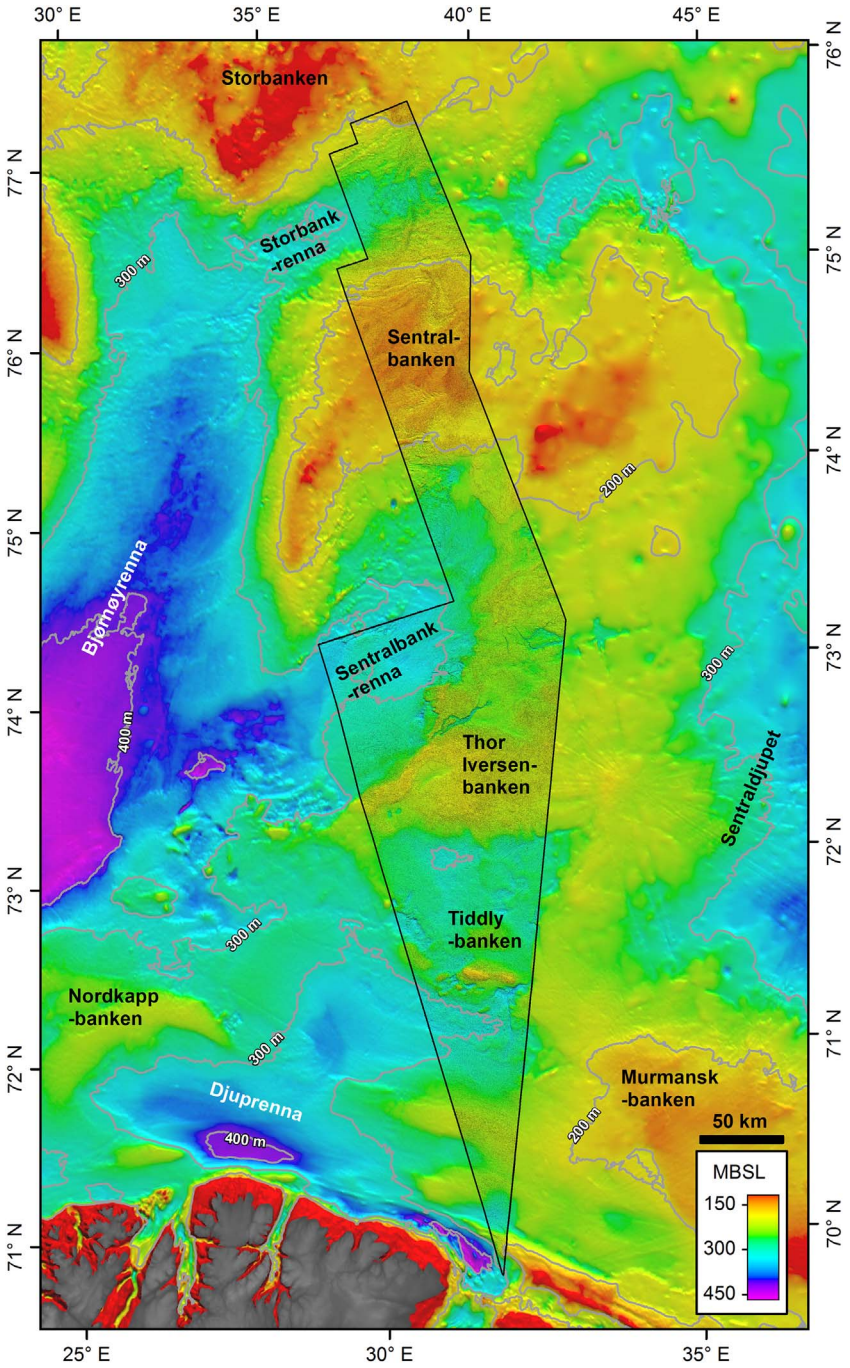

Fig. 3. The bathymetric survey in the study area is overlain ontop of the IBCAO v.3.0 (Jakobsson et al., 2012b). Place names are also labelled for reference to subsequent figures and text. MBSL means metres below sea level. These abbreviations are the same for all subsequent figures.

(Fig. 4c) have been overlain by ridge deposits and show a WSW-ESE orientation. These MSGLs probably represent the earliest period of ice flow through Storbankrenna into Bjørnøyrenna and pre-date the MSGLs formed during the later advance (Fig. 4a). The MSGLs in Sentralbank-renna (Fig. 4d) show an arcuate orientation that is parallel to the trough; suggesting fast-flowing ice was guided by the topography. MSGLs near Tiddlybanken suggest NE-SW oriented ice stream flow (Fig. 4e). Many MSGLs show a relationship with adjacent wedges and this is fully discussed in Section 4.6. The observed flow patterns correspond well with previous flow patterns inferred from less extensive high-resolution data (Bjarnadóttir et al., 2014).

4.2. Channels

In Storbankrenna, a 38 km long, ~100 m wide, and 10–15 m deep channel is observed (Fig. 5a). On Thor Iversen-banken channels are larger and show dendritic and braided patterns. Channel 2 is dendritic with widths and depths of 500–800 m and 8–22 m, respectively (Fig. 5b). Regional bathymetry shows the channel continues out of the survey area (Jakobsson et al., 2012b). Channel 3 is ~60 km long with similar dimensions to Channel 2 (Fig. 5c). It cuts through a set of moraines described in Section 4.4 and terminates at the slope of Sentralbankrenna (Fig. 5c).

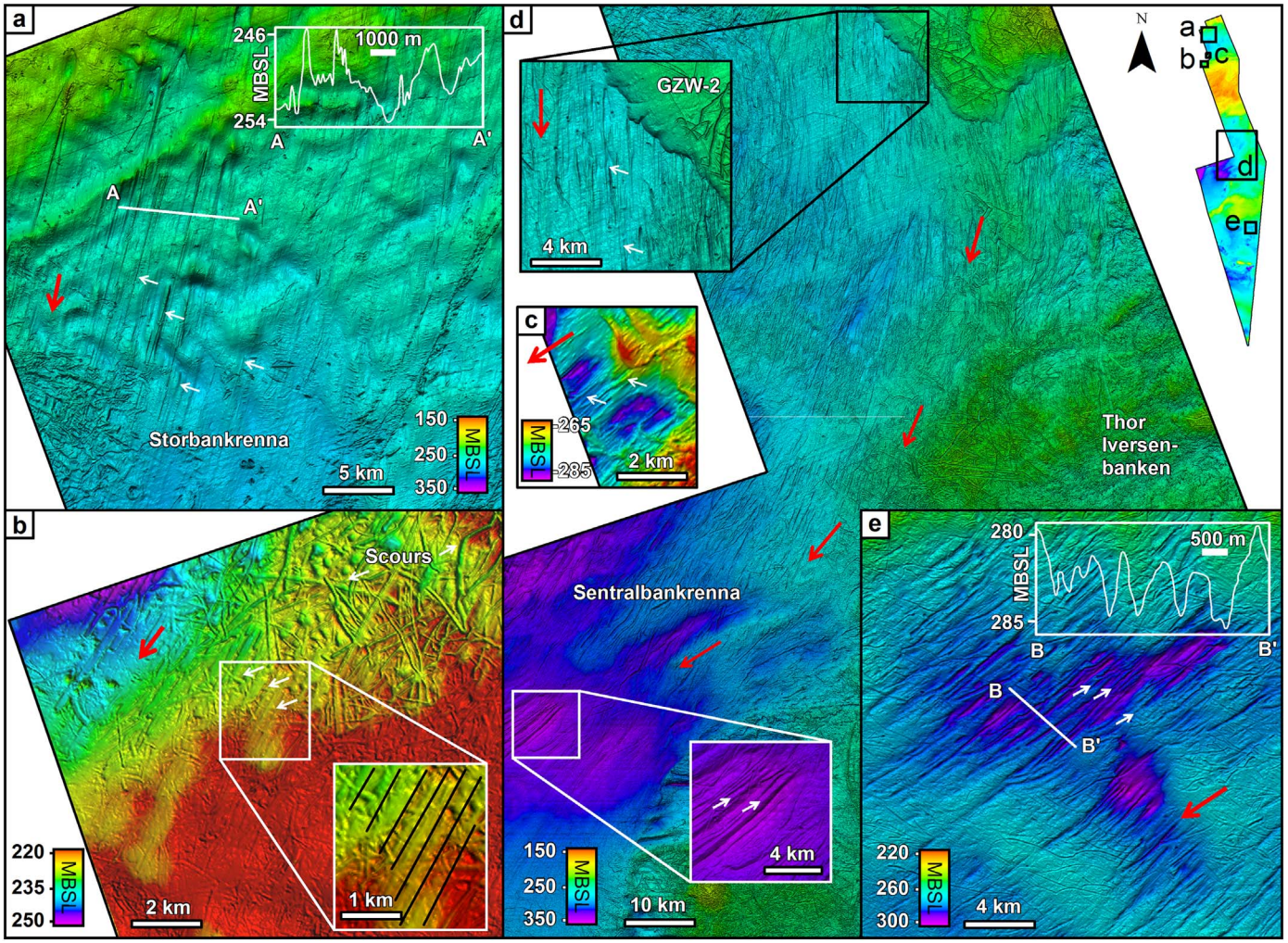

Fig. 4. Examples of mega-scale glacial lineations (MSGLs) with associated elevation profiles across the survey; a) MSGLs that cross-cut a ridge in Storbankrenna; b) a continuation of the MSGLs observed in (a) but heavily disrupted by iceberg scours; c) MSGLs related to the earliest conditions of ice streaming in Storbankrenna. The MSGLs have been partially buried by retreat moraines; d) MSGLs in Sentralbankrenna showing ice flow pathway. The upper inset panel shows the apparent continuation of the MSGLs beneath the grounding-zone wedge. These MSGLs have been partially imaged by Bjarnadóttir et al. (2014) in the area of the lower inset; e) MSGLs in the southern part of the survey to the north of Tiddlybanken. In each panel the white arrows point to individual lineations and the red arrows show the dominant orientation and inferred ice flow pathway. (For interpretation of the references to colour in this figure legend, the reader is referred to the web version of this article.)

Channel 4 is 20 km long, 200–300 m wide, and has a depth range of 10–50 m (Fig. 5c). Channel 5 is ~50 km long and terminates at Sentralbankrenna. It is characterised by braiding and an overdeepening (Fig. 5d). Channel 6 is adjacent to Tiddlybanken and is observed as an overdeepened channel ~60 km long, 0.8–2.5 km wide, and up to 50 m deep (Fig. 5e). In the larger channels (2 and 4–6) the thalwegs have an undulating basal topography.

These channels are interpreted as tunnel valleys, which are long and often steeply-flanked, overdeepened subglacial drainage pathways (Ó Cofaigh, 1996; Huuse and Lykke-Andersen, 2000) with a typical width-to-depth ratio of 1:10 (van der Vegt et al., 2012). The width-to-depth ratios observed here range from 1:10 (Fig. 5a–d) to 1:40 (Fig. 5e). The geometries of the tunnel valleys in the central Barents Sea fall comfortably within those described elsewhere (van der Vegt et al., 2012). The undulating thalwegs also indicate that the channels are tunnel valleys since the water was able to flow upslope (Fig. 5c, d). This is because the hydraulic gradient of a tunnel valley is controlled by the ice surface slope, meaning that subglacial meltwater can flow upslope (Ó Cofaigh, 1996).

Tunnel valley 1 (TV-1) in Storbankrenna cross-cuts a number of MSGLs; this suggests that the tunnel valley postdates the MSGLs (Fig. 5a). However, although the presence of meltwater and inefficient drainage at the base of an ice stream are known to aid ice streaming (Engelhardt and Kamb, 1997; Kyrke-Smith et al., 2013), a coeval formation cannot be currently ruled out as channelised and efficient meltwater discharge has been observed below Antarctic ice streams (Le Brocq et al., 2013). TV-2 and TV-3 on Thor Iversen-banken terminate at the lateral margin of Sentralbankrenna and probably mark the confluence of slower-moving ice from the bank with the ice stream in the trough (Fig. 5b, c). TV-4 (Fig. 5c) on Thor Iversen-banken overdeepens as a number of coalescing valleys increased water volume and velocity sufficiently that the substrate was further incised, implying that the substrate was more easily erodible. Retreat moraines (Fig. 5c) cut by the tunnel valley, imply that TV-4 is a younger feature. However, if the tunnel valley is older, ongoing drainage could have prevented material accumulating and infilling the tunnel valley.

The base of TV-5 is characterised by a braided and undulating topography (Fig. 5d). It is not clear how much of this is due to bedrock restriction of valley width, but the relatively large width suggests that the location of meltwater discharge may have been stable for a significant period of time. Thalweg undulations and braiding also suggests that discharge was variable through time (Ó Cofaigh, 1996; Huuse and Lykke-Andersen, 2000). An area of homogenous low-relief upstream of TV-5 (Fig. 5d) may represent a local basin where meltwater accumulated and fed

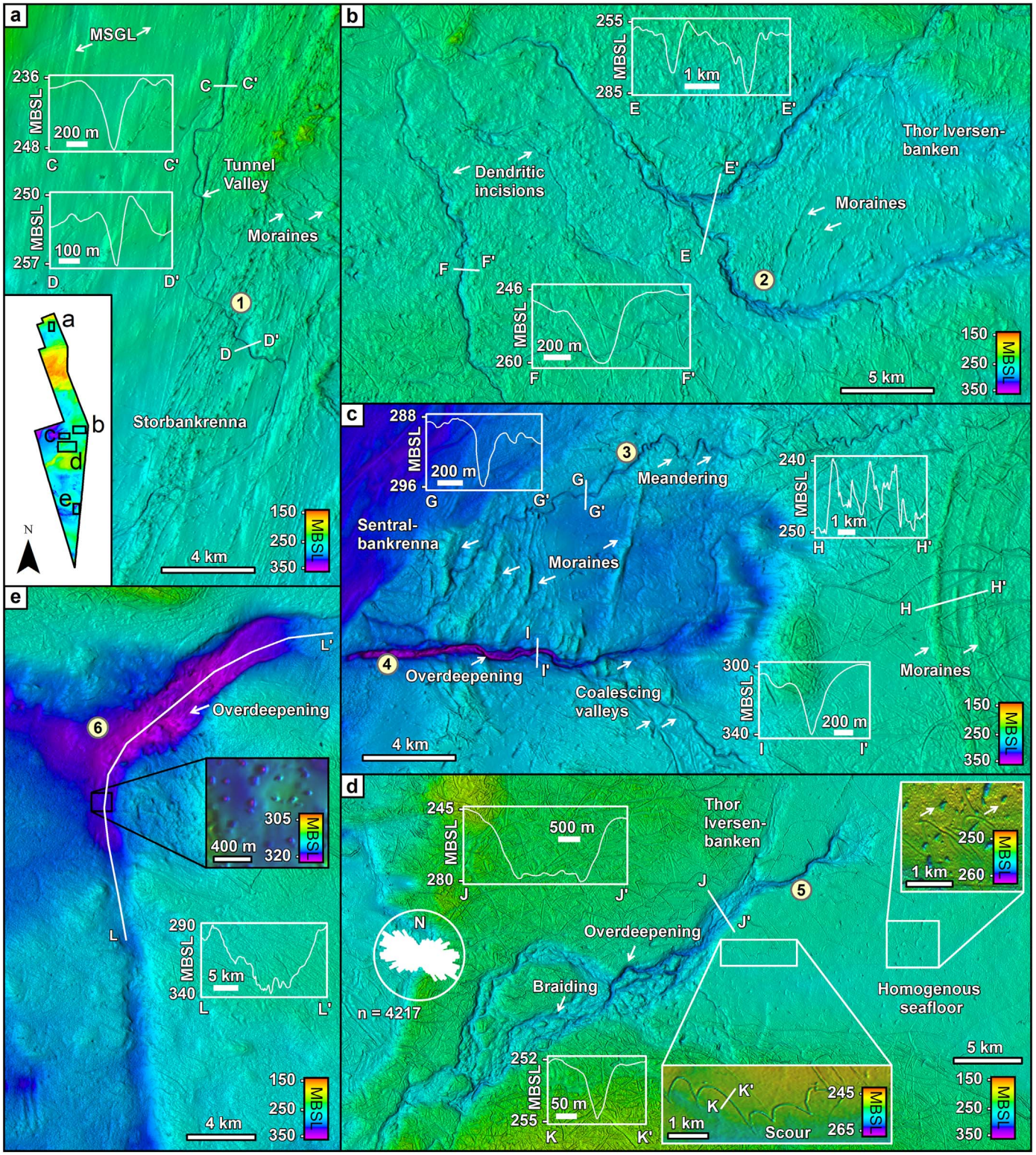

Fig. 5. Multiple examples of tunnel valleys and profiles across the survey area; a) tunnel valley 1 (TV-1) with associated MSGLs and retreat moraines in Storbankrenna; b) TV-2 and its tributary network on Thor Iversen-banken. Retreat moraines are also observed; c) the smaller valley in the north is TV-3 and the larger, overdeepened valley in the south is TV-4. Multiple retreat moraines are also observed on Thor Iversen-banken and are indicated by the white arrows; d) TV-5 on the southern part of Thor Iversen-banken. Inset panels show a curvilinear iceberg scour and observations of iceberg grounding pits; e) TV-6 is located between Thor Iversen-banken and Tiddlybanken. The inset panel shows observations of pockmarks associated with fluid expulsion.

the tunnel valley, perhaps catastrophically when subglacial pressures were too high. Further data is required to fully elucidate this hypothesis, but similar landform assemblages have been described in Canada (Livingstone et al., 2016). TV-5 terminates at the margin of Sentralbankrenna and may have been an important source of lubricating meltwater to the ice stream bed. In Tiddlybanken, TV-6 is significantly deeper than the other tunnel valleys and it occurs in a wide area of low topography that may represent a local basin of meltwater accumulation (Fig. 5e).

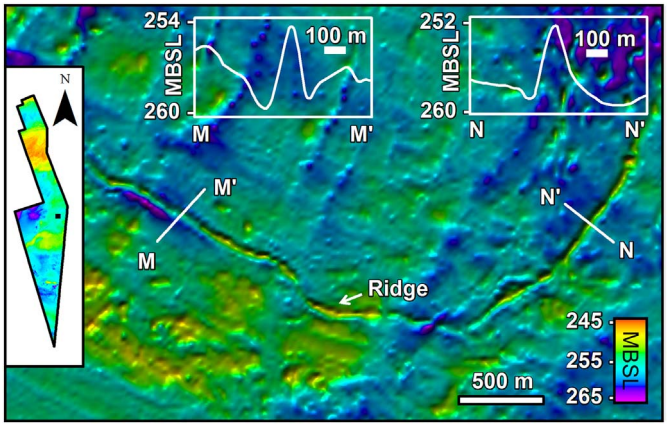

Fig. 6. A sinuous ridge that has been interpreted as a subglacially formed esker.

4.3. Sinuous ridge

A ~4 km long sinuous ridge (Fig. 6) is located adjacent to TV-2 (Fig. 5b). The ridge is 2–5 m high, 100–120 m wide, and is roughly orientated orthogonal to the Sentralbankrenna trough and to local observations of retreat moraines (see Section 4.4). Eskers are long, sinuous ridges formed in subglacial and englacial ice-walled conduits (Banerjee and McDonald, 1975; Henderson, 1988). Upon glacier recession or ice down-wasting, these channels leave behind ridges of stream deposits that are typically up to 50 m high, 100–200 m wide, and a few kilometres long (Storrar et al., 2014). This ridge is interpreted as an esker and indicates efficient subglacial drainage (Röthlisberger, 1972; Shreve, 1985), as is also suggested by TV-2 (Fig. 5b). Ottesen et al. (2008a) suggested that englacial and subglacial eskers can be distinguished, as englacially-formed eskers are likely to have a more disturbed appearance as they may be deposited on the seafloor in a more chaotic, time-transgressive manner. This esker is thought to have formed subglacially because its smooth topography suggests that meltwater gradually cut into the ice above. Although it is difficult to

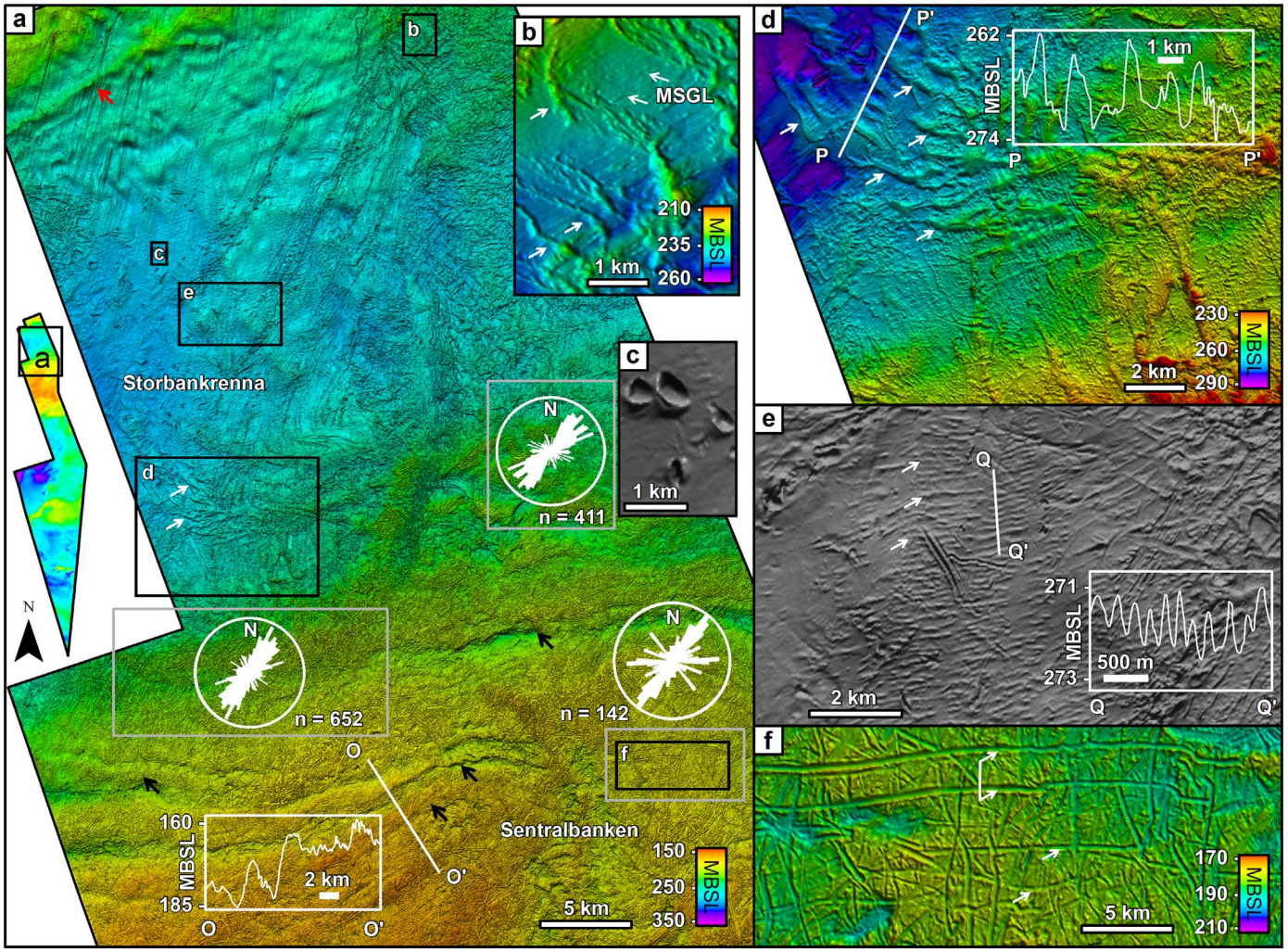

Fig. 7. a) red and black arrows point to large-scale ridges that have been interpreted as moraines. White arrows indicate smaller retreat moraines. The rose charts show the orientation of iceberg scours within each of the three grey boxes. Subsequent locations of other panels are indicated; b) examples of smaller ridges showing retreat of the ice margin that is superimposed on MSGLs indicated the earliest ice flow pathway through Storbankrenna; c) shaded-relief image showing observations of iceberg grounding pits and the adjacent deposit of excavated material; d) retreat moraines, possibly annual push moraines, are indicated by the white arrows; e) shaded-relief image showing small ridges indicated by the white arrows and associated elevation profile have been interpreted as retreat moraines, possibly De Geer-type moraines from a tidewater glacier margin; f) examples of iceberg scours on Sentralbanken. The white arrows indicate individual iceberg scour examples and the double-headed white arrow indicates a double-keeled iceberg. (For interpretation of the references to colour in this figure legend, the reader is referred to the web version of this article.)

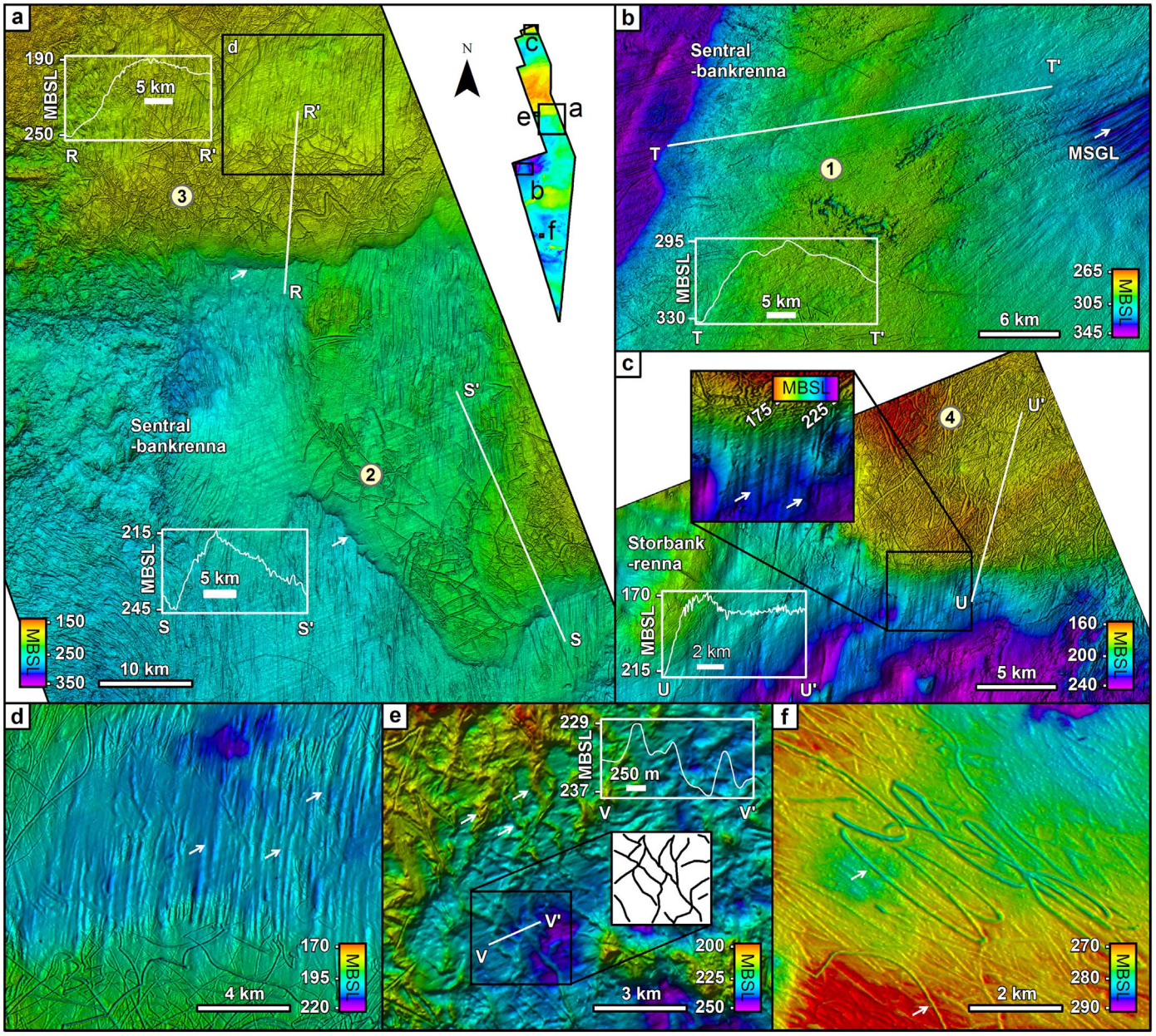

Fig. 8. a) sequence of grounding-zone wedges (GZWs) deposited on top of each other with MSGLs superimposed on top of each GZW in Sentralbankrenna. The location of panel (d) is shown; b) large GZW accumulated at the western margin of Sentralbankrenna accumulated during a period of stillstand; c) possible GZW at the northernmost edge of Storbankrenna. GZW described in the text numbered from south to north; d) observations of MSGLs on GZW-3 in Sentralbankrenna. Arrows point to examples of MSGLs; e) reticulated (or rhombohedral) pattern of ridges in Sentralbankrenna that have been interpreted as crevasse-squeeze ridges. The inset panel shows a small number of digitised ridges to display the reticulated pattern; f) example of chaotic scour in the area between Tiddlybanken and Thor Iversen-banken.

determine a time of formation relative to other landforms, the ridge is within close proximity to a network of crevasse-squeeze ridges (see Section 4.7), suggesting coeval formation during a period of ice stagnation.

4.4. Ridge features

A number of ridges are observed in Storbankrenna (Fig. 7a, b, d) and Thor Iversen-banken (Fig. 5c). Ridges in Storbankrenna are 4–55 km long, 1–4 km wide, and 5–20 m high. The ridge in the northwest of the survey (red arrow in Fig. 7a) has MSGLs superimposed on its crest (Figs. 4a, 7a), suggesting that it was overridden by grounded ice after its formation. On the southern side of Storbankrenna, several ridges similar in size are recorded (black arrows in Fig. 7a). In between the two sets of large ridges, smaller ridges are observed and are typically 0.5–4 km long, 200–600 m wide, and 5–8 m high (Fig. 7b, d). These ridges are deposited on top of the early and readvance MSGLs (Figs. 4c, 7b) and are typically orthogonal to the latter. On Thor Iversen-banken, ridges are observed and cut by iceberg scours and tunnel valleys (Fig. 5c). These arcuate ridges are 5–10 m high, 400–800 m wide and 10–14 km long.

Although subsurface data is required to rule out that the ridges are bedrock features, the rugged topography generated by iceberg scouring suggests that the ridges are, at least in the upper-most part, sedimentary in origin. The large size of the prominent ridges in Storbankrenna suggests that they are moraines that mark the former ice sheet margin (Fig. 7a). The length of time taken for formation depends on the flux of material to the margin, but their relatively large size implies the ice sheet margin may have been stable at each moraine for a significant period of time, perhaps at least a few decades.

MSGLs in Storbankrenna suggest the northernmost moraine was overridden by ice (Fig. 4a and red arrow in Fig. 7a), whereas the four large moraines in the south (black arrows in Fig. 7a) and the smaller moraines recorded in between (Fig. 7d) lack such evidence. This suggests that ice did not advance beyond this point during the readvance (Fig. 7a). The smaller ridges recorded in Storbankrenna are interpreted as retreat moraines, possibly annual push moraines, formed by small advances during the overall retreat of the ice margin (Fig. 7b, d) (Boulton, 1986). This suggests that the ice margin was retreating episodically (Dowdeswell et al., 2008). Given the similarity in both the geometry of the ridges and the likelihood that they were formed in a tidewater glacier setting, these ridges are similar to De Geer moraines observed in Sweden and Canada (Lindén and Möller, 2005; Todd et al., 2007).

On Thor Iversen-banken, the ridges are interpreted as retreat moraines (Fig. 5b, c). These are located on the bank area adjacent to Sentralbankrenna and their orientation is not orthogonal to the MSGL-inferred ice flow pattern observed in the trough (Fig. 4d). This suggests that prior to deglaciation this area probably marked the confluence of ice from the west across Thor Iversen-banken into Sentralbankrenna. During retreat of ice through the trough the moraines suggest that the ice on Thor Iversen-banken uncoupled from the ice stream in Sentralbankrenna. The Thor Iversen-banken ice cover then retreated to the east, with several stillstands, as the ice in Sentralbankrenna retreated through the trough to the different grounding-zones wedges (see Section 4.6). In general, the small ridges are uncommon compared to other locations nearby where they are more prominent on the bank areas (e.g. Bjarnadóttir et al., 2014), possibly owing to better preservation potential as large areas of the banks observed here are heavily iceberg scoured (see Section 4.8).

4.5. Parallel ridges

In Storbankrenna a set of highly-uniform ridges are transverse and superimposed on top of the MSGLs (Fig. 7e). The ridges are typically 0.4–3 km long, 100–150 m wide, 0.4–2 m high, and have a wavelength between ridge crests of 130–140 m. These features appear similar to corrugation ridges described in Antarctica (Jakobsson et al., 2011) and the Barents Sea (Andreassen et al., 2014; Bjarnadóttir et al., 2014). They are thought to form during tidally-modulated sea level changes and periodic grounding of mega-icebergs or ice shelf keels that are close to floatation (Jakobsson et al., 2011; Graham et al., 2013). Corrugation ridges are also typically observed in adjacent iceberg scours. However, this is not the case here and no ridges are observed in adjacent iceberg scours. Ridge dimensions are similar to the small moraines described in Section 4.4 and are interpreted as retreat moraines. This suggests retreat of a tidewater ice margin in Storbankrenna was punctuated by brief, possibly annual, advances or stillstands of the ice margin. The good preservation of MSGLs (Fig. 4a) implies that ice was probably cold-based and unable to significantly rework these deposits.

4.6. Asymmetric wedges

A number of wedges are observed in the Sentralbankrenna and Storbankrenna troughs. The three largest wedges (wedges 1–3) have an asymmetric shape (with the steepest side dipping to the west for wedge 1 and to the SSW for wedges 2 and 3) (Fig. 8a–c). The wedges rise 30–60 m above the local seafloor and are several tens of kilometres wide (measured orthogonal to the trough axis), covering an area of at least ~1800–3500 km^2 (the wedges clearly continue outside the survey) (Fig. 8a, b). A smaller wedge (wedge 4) is observed in Storbankrenna (Fig. 8c) and although it is not clear on the regional bathymetry (Jakobsson et al., 2012b) (Fig. 1a), the part contained within the survey shows a similar asymmetric shape that is ~40 m high, 15–20 km wide, and covers at least ~750 km^2 (Fig. 8c). Relative ages of wedges 2 and 3 can be derived through the superposition of wedge 3, suggesting it is younger (Fig. 8a).

These wedges are interpreted as grounding-zone wedges (GZW) based on their morphology, asymmetric shape, and relationship to the MSGLs (Fig. 8a–c). Similar landform assemblages are present in studies near the survey area (Andreassen et al., 2014; Bjarnadóttir et al., 2014) and on other glaciated margins (Dowdeswell et al., 2016). GZWs are typically composed of diamictic subglacial debris and ice-contact deposits that have been delivered to the grounding-line and indicate that ice margin retreat was punctuated by stillstands during deglaciation (Dowdeswell et al., 2008). The asymmetric shape of the GZWs, with the steep lee-side orientated downstream (Batchelor and Dowdeswell, 2015), shows that ice was flowing predominantly from NNE to SSW in Storbankrenna and the upper part of Sentralbankrenna (Fig. 8a, c), which is in agreement with the MSGLs record. GZW-1 indicates that ice flow was ENE-WSW in outer Sentralbankrenna (Fig. 8b). This change in direction from GZW-1 to GZW-3 is recorded in the intervening area by the MSGLs.

MSGLs in Sentralbankrenna (GZW-2 and GZW-3) appear to continue below and above the GZW with similar orientations; suggesting fast-flowing ice across the area prior to, and during, the formation of the GZWs (Figs. 4d, 8d). This indicates that ice flow direction changed little as ice retreated between GZW-2 and GZW-3. The preservation of MSGLs also suggests that the retreat between each GZW was sufficiently rapid that the MSGLs were not significantly reworked by grounded ice or a collapsed ice shelf. MSGLs also appear to continue beneath GZW-4 (Fig. 8c), but extensive iceberg scouring means that if they were present on top of the wedge they have been reworked. GZWs are thought to take decades to centuries to form (Dowdeswell and Fugelli, 2012), meaning that between the phases of rapid retreat the ice sheet margin remained stable, possibly with an ice shelf, whilst material accumulated at the grounding-line. The interpretation of episodic retreat fits well with previous interpretations of adjacent landform records in the central Barents Sea and Bjørnøyrenna (Andreassen et al., 2014; Bjarnadóttir et al., 2014).

4.7. Reticulated ridges

In water depths of ~270 m in Sentralbankrenna, a reticulated (or rhombohedral) pattern of 0.5–2 km long, < 100–150 m wide, and 3–6 m high ridges is observed (Fig. 8e). There is some evidence of iceberg scouring, but the berms and associated furrows are clearly distinguishable from the reticulated ridges. Where iceberg scouring is more prevalent the distinction is more difficult due to extensive reworking. Although similar ridges are observed in Storbankrenna, elsewhere in the survey these patterns are uncommon because they were either not formed or are not preserved.

The ridge networks are similar to crevasse-squeeze ridges (CSRs) observed in front of surge-type glaciers on Svalbard (Ottesen and Dowdeswell, 2006; Flink et al., 2015). In areas of high velocity ice flow, deformable beds and water-saturated sediments are common and provide the initial conditions for injection of debris into basal crevasses due to the overburden pressure (van der Veen, 1998; Evans and Rea, 1999). The CSRs are then preserved on the former bed of the ice when the margin stagnates and down-wastes or lifts-off without reworking the CSRs through increased buoyancy. The MSGLs described in Section 4.1 indicate fast-flowing ice in Sentralbankrenna, whilst the CSRs indicate stagnation and uncoupling of the ice from the bed as the grounding-line migrated upstream. Rapid uncoupling of the ice from the seabed is required so that downstream flow does not rework the CSRs (Andreassen et al., 2014).

4.8. Curvilinear grooves

Linear and curvilinear grooves occur across the majority of the survey but are less common (when compared to the bank areas) in water depths > 300 m. Grooves are generally < 5–10 km in length

(Fig. 5d) with the longest grooves measured at ~50 km. Grooves are generally characterised by sharply-defined furrows with adjacent berms that are up to 14 m deep (Figs. 5d, 7f). Cross-cutting of these grooves means that they are often segmented and may be longer. The longest grooves are more common west of Sentralbankrenna and Tiddlybanken. Widths are typically 100–300 m but may measure up to 600 m. The grooves are interpreted as iceberg scours because of their similar morphologies to scours described elsewhere (Bass and Woodworth-Lynas, 1988; Syvitski et al., 2001). The scours are formed when an iceberg keel penetrates soft, unconsolidated sediments to leave behind linear and curvilinear grooves as the iceberg is moved by ocean currents or winds.

Scour orientations vary considerably and frequently cross-cut each other. On a local level, such as on the slope between Storbankrenna and Sentralbanken, NE-SW scour orientations suggest that icebergs grounded as they moved up onto the bank areas (Fig. 7a). On Thor Iversen-banken WNW-ESE trajectories suggest that the icebergs may have moved from the trough area and grounded on the bank as the ice margin retreated between the GZW-1 to GZW-3 (Fig. 5d). Conversely, the lack of scouring on the area of homogenous topography on Thor Iversen-banken suggests that it was likely ice covered when the scours were formed. This ice cover might have produced icebergs that scoured Thor Iversen-banken as they moved away from the calving front toward Sentralbankrenna. In Sentralbankrenna, the area of GZW-1 is reworked by the longest and widest iceberg scours. These larger scours regularly cross-cut narrower scours in the area and typically have a less sharply defined base, suggesting that the thicker iceberg scours represent the greater availability of wider deep-draft icebergs. This might be related to a possible collapse, or increased calving flux, of the ice stream front as the margin retreated from GZW-1 to GZW-2.

Observations of iceberg scours with spiral or arcuate trajectories (Fig. 5d) show the combined influence of geostrophic (possibly the North Atlantic Current) and tidal currents on iceberg trajectory (Newton et al., 2016). Chaotic scours which repeatedly change direction (Fig. 8f) are likely related to iceberg overturning or localised currents related to subglacial drainage that prevent the iceberg from moving away. Double-keeled icebergs are also observed on Sentralbanken (Fig. 7f). Isolated pits 5–10 m deep and 100–300 m wide (Figs. 5d, 7c), have been formed by icebergs that experienced temporary grounding during either low tidal conditions, or perhaps from the momentary passing of ocean swell (Bass and Woodworth-Lynas, 1988). These pits (Fig. 5d) are generally much larger than the pockmarks (Fig. 5e) described in Section 4.9.

Most of the iceberg scours have cut other glacial landforms, meaning that they are younger features. Determining the precise chronology of when cross-cutting occurred is difficult because iceberg calving occurs under retreating and stable margin conditions. Taken together, landforms indicating retreat (e.g. moraines) and the extensive iceberg scouring in the deepest areas (i.e. the availability of deep-draft icebergs) suggest that the scouring occurred during retreat of the ice sheet between stillstand locations. The shallower bank areas were probably reworked throughout the time period once they were free of grounded ice.

The scours are generally restricted to contemporary water depths of 140–300 m. The LGM sea level is thought to have been ~130 m lower than the present (Lambeck et al., 2014), suggesting that the icebergs that scoured the area would have had drafts of ~10–170 m. Whilst raised beaches on Svalbard are up to 100 m above sea level (Forman et al., 1995), the post-glacial marine limit on Novaya Zemlya is ~15 m above sea level (Zeeberg et al., 2001). This dichotomy between the relative sea level changes either side of the Barents Sea implies that the major ice load was located over the central and northern Barents Sea, causing a crustal depression of ~100–200 m at the LGM (Landvik et al., 1998; Patton et al., 2016). Assuming that sea level rise was at least matched by isostatic rebound as the ice sheet lost mass, iceberg drafts were probably ~200–400 m.

4.9. Seafloor craters

In the Sentralbankrenna trough and south of Tiddlybanken, there is a high density of circular craters on the seafloor (Fig. 5e). These craters have a more rounded morphology than the iceberg pits described above and lack the adjacent excavated material (Fig. 7c). They are generally ~5 m deep and 20–40 m in diameter. These craters have been interpreted as pockmarks caused by the fluid expulsion due to their rounded morphology and the general lack of adjacent iceberg scours that would be expected if iceberg pits were so prevalent (Andreassen et al., 2007; Brown et al., 2017).

4.10. Landform assemblages and flow-sets

The landform record described above was digitised and generalised into flow-sets (Fig. 9), where a set or an assemblage of landforms summarise a single ice sheet phase or event in the central Barents Sea (e.g. stillstand or ice streaming). The rationale for determining each flow-set is described in Table 1. The different flow-sets derived from the landform assemblages and their cross-cutting relationships are assumed to reflect a time transgressive record of the evolving ice sheet margin. Without geochronological data, it is assumed that margins retreated at similar rates, and thus, that some flow patterns may have been coeval in time.

5. Discussion

5.1. Deglaciation of the survey area

Ice dynamics across the survey have not been reconstructed in the southern-most area because of the limited areal extent of the data. Previous studies in this area have shown several phases of ice margin stillstand, stagnation, and fast-flow reactivation during the deglaciation after the LGM (Winsborrow et al., 2010; Bjarnadóttir et al., 2014). This is considered in Section 5.2. In this section, the spatio-temporal glacial evolution has been tentatively reconstructed in a number of successive times-slices for the Storbankrenna and Sentralbankrenna troughs, and adjacent bank areas (Fig. 10).

At the LGM, MSGLs suggest that smaller ice streams in Storbankrenna (Fig. 4c) and Sentralbankrenna (Fig. 4d) are thought to have flowed into the main trunk of the Bjørnøyrenna Ice Stream (Bjarnadóttir et al., 2014). As the Bjørnøyrenna Ice Stream retreated after the LGM, it stabilised at a number of positions in the Bjørnøyrenna Trough (Andreassen et al., 2014; Bjarnadóttir et al., 2014). Concomitant with this retreat, MSGLs and GZW-1 indicate that a smaller ice stream was no longer confluent with the Bjørnøyrenna Ice Stream and stabilised in the Sentralbankrenna trough (Figs. 4d, 8b, 10a). Thus, the Bjørnøyrenna Ice Stream was no longer being fed by the Sentralbankrenna Ice Stream, but only by ice flowing southward, likely from an ice divide over Storbanken and Svalbard. Tunnel valleys incised into Thor Iversen-banken (Fig. 5b–d) terminate at the boundary between the bank area and Sentralbankrenna and the availability of meltwater discharging directly into the trough may have provided lubrication to the ice stream base and in combination with topographic restriction of ice flow and a deformable substrate, helped to drive fast-flowing ice through Sentralbankrenna.

MSGLs in Sentralbankrenna (Fig. 4d) indicate an arcuate flow path of the ice stream that was topographically constrained in the trough as it rapidly retreated from GZW-1 to GZW-2 and then GZW-3 (Figs. 8a, 10b). MSGLs appear to continue below the wedges and are also present on the top of each GZW; suggesting fast-flowing ice prior to and after retreat between each GZW. The MSGLs, GZW-2, and GZW-3 suggest that the fast-flowing ice retreated to the northeast (Fig. 10b). CSRs observed to the west of GZW3 (Fig. 8e) suggest that the ice cover here had become stagnant before mass loss eventually led to rapid uncoupling from the seafloor. Moraines on the bank area then indicate slow

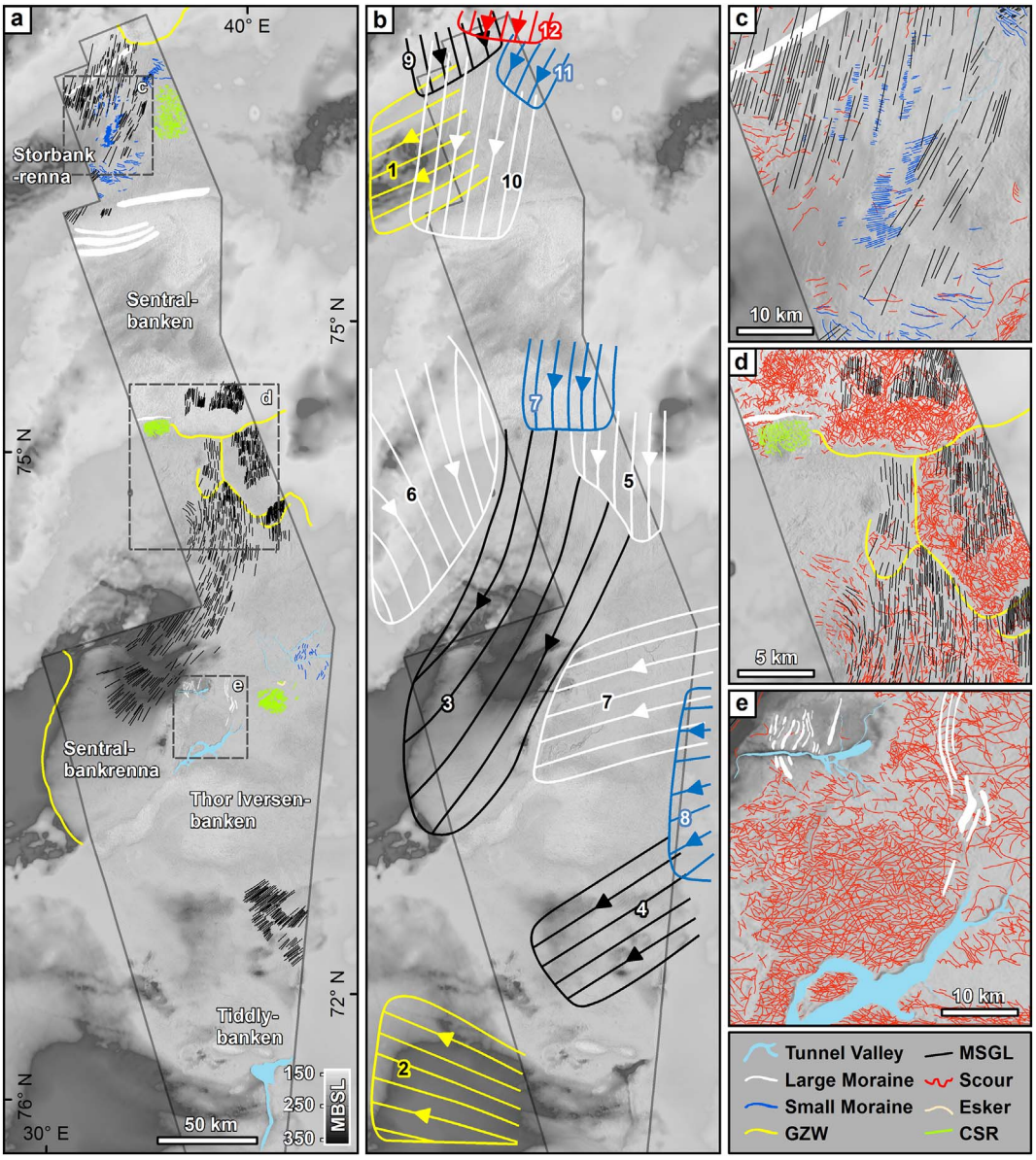

Fig. 9. a) detailed bathymetry overlain onto regional IBCAO v.3.0 bathymetry (Jakobsson et al., 2012b). The large-scale record of landforms is presented without iceberg scours for clarity due to the large number that are present; b) generalised flow-sets derived from the geomorphological record - descriptions and rationale of each flow-set are described in Table 1. The colours of the flow-sets are to allow differentiation of each flow-set and do not imply a link to other flow-sets with the same colour; c) enlarged image of the landform assemblage in the Storbankrenna; d) enlarged map showing retreating grounding-zone wedges in Sentralbankrenna; e) enlarged image of features on Thor Iversen-banken; cross-cutting of flow-sets represent the relative chronology of each set of landforms. Abbreviations are as follows: crevasse-squeeze ridges (CSR), grounding-zone wedge (GZW), and mega-scale glacial lineation (MSGL). (For interpretation of the references to colour in this figure legend, the reader is referred to the web version of this article.)

retreat of the margin to the northwest onto Sentralbanken (Bjarnadóttir et al., 2014). These retreat patterns appear to show that ice retreat was topographically-driven as grounding-lines retreated in different directions to higher elevations across Sentralbanken. Such an interpretation is in agreement with adjacent landforms (Bjarnadóttir et al., 2014). Additional data is required to the east of the survey to elucidate if ice was still fast-flowing as it retreated behind GZW-3.

As the ice margin retreated through Sentralbankrenna, the ice stream likely uncoupled from the ice on Thor Iversen-banken along the eastern break of slope in the trough (Fig. 10c, d). Retreat moraines (Fig. 5c) suggest that ice was grounded and episodically retreating as the ice margin moved southeast across Thor Iversen-banken (Fig. 10c, d). It was suggested earlier that TV-3 and TV-4 could pre-date or post-date moraine formation, however, if the moraines were deposited first, then it would have required that they were not reworked during a subsequent ice advance when the tunnel valleys were formed. The moraines are well-preserved and do not appear to be heavily modified, suggesting that a subsequent advance over the moraines is unlikely. If the tunnel valleys were operational at the ice terminus after the ice masses uncoupled, then this would have prevented the build-up of material in the incision as ice retreated. Therefore, it is interpreted that tunnel valley formation pre-dates the retreat moraines as this better fits with the ice dynamics described above. CSRs on Thor Iversen-banken suggest further down-wasting and rapid lift-off at the ice margin as it retreated to the east (Fig. 10c). The ice margin continued to retreat and deposited a number of retreat moraines (Fig. 9a) before the ice margin moved out of the survey area.

No studies of high resolution bathymetric data to the east of Thor Iversen-banken and Tiddlybanken have been published, but it seems likely that the ice margin retreated toward Sentraldjupet and Murmanskbanken (Polyak et al., 1995; Svendsen et al., 2004; Bjarnadóttir et al., 2014). As is indicated by the retreat pattern

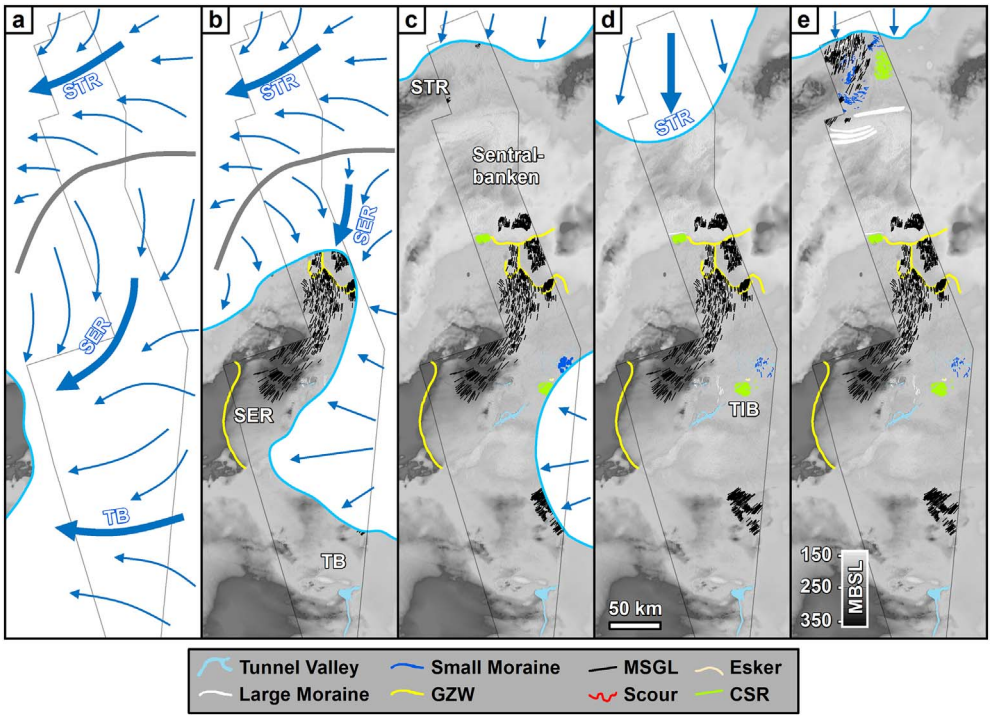

Fig. 10. Reconstruction of the demise of the central part of the BSIS across a number of tentative time-slices between 16 and 14 ka (a–e). Ice sheet margins and flowlines are based on the landform analysis in this paper, as well as published work on the adjacent areas (Winsborrow et al., 2010; Bjarnadóttir et al., 2014) but are necessarily schematic for areas due to the lack of dating control with which to constrain the chronology. The landform records that have been left behind after each event are also overlain onto the bathymetry. The white polygon marks the ice sheet extent and the thick blue arrows show areas where evidence for fast-flowing ice is observed. The thinner blue arrows show a generalised ice flow pattern based on the landform analysis, as well as an intuitive interpretation of the likely ice flow patterns in response to the topographical setting. The grey lines highlight possible ice divide locations that honour these flow patterns. Abbreviations are the same as for Figs. 1 and 9. The blue outlined abbreviations are the same but refer to the ice streams discussed in the text. See Fig. 2 for location. (For interpretation of the references to colour in this figure legend, the reader is referred to the web version of this article.)

described above, after the ice margins uncoupled, retreat became topographically-controlled as grounding-lines moved to higher elevations on the bank areas. This interpretation is in agreement with the suggestion of Bjarnadóttir et al. (2014) that local ice divides may have developed over the bank areas as the deglaciation progressed.

As ice on Thor Iversen-banken and Tiddlybanken began to act independently, so did the ice cover further to the north (Fig. 10c). The ice stream in Storbankrenna that was previously confluent with the Bjørnøyrenna Ice Stream was no longer present as the ice margin had retreated to the northernmost moraine (red arrow in Fig. 7a). MSGLs suggest that the ice margin was grounded as it advanced over the moraine (Figs. 4a, 10d). The readvance was possibly associated with a reduction in backstress of the margin due to sea level rise and/or ice sheet thinning. The loss of backstresses have been shown on the Antarctic Peninsula to have resulted in the speed up in glacier velocity after the collapse of the Larsen B ice shelf (Rignot et al., 2004; Scambos et al., 2004); a similar change in stress regime here may have resulted in the readvance of the margin in the central Barents Sea.

The southern moraines (black arrows in Fig. 7a) indicate that backstresses increased and the margin stabilised on the northern flank of Sentralbanken. After deposition of the larger moraines to the south, the frequent deposition of smaller retreat moraines indicates that the ice margins were stable for shorter periods of time (Fig. 7d, e). The tunnel valley observed here (TV-1) cross-cuts the MSGLs and indicates a more channelised subglacial drainage after the readvance. It is possible that this tunnel valley indicates a switch from a distributed to a channelised subglacial flow regime that may have contributed to the slowdown of ice stream velocity and subsequent stagnation. However, additional acoustic stratigraphic data are required to test this hypothesis. Buoyancy increases through ice sheet thinning and/or sea level rise then led to the rapid floatation of the stagnant ice margin permanently, leaving behind a network of CSRs (Fig. 9a). The accumulation of GZW-4 also provides evidence that an ice shelf may have been present (Figs. 8c and 10e). Evidence for late Weichselian ice flow to the southwest from Storbanken to Storbankrenna is also observed (Bjarnadóttir et al., 2014). This fits well with the deglaciation pattern described here as an ice divide prevailed over Storbanken. This cyclical behaviour between fast- and slow-flowing ice has also been described for the nearby Bjørnøyrenna Ice Stream (Andreassen and Winsborrow, 2009; Andreassen et al., 2014; Bjarnadóttir et al., 2014).

5.2. Deglaciation of the central Barents Sea

Dating studies in the Barents Sea suggest that the BSIS separated from the FIS in the central Barents Sea sometime between 17.5 and 11.1 cal. ka BP (Salvigsen, 1981; Polyak et al., 1995; Rüther et al., 2011). In order to reconstruct ice margin evolution through the period of separation, the findings of this paper (Fig. 10) have been integrated with datasets from other studies. The 'most-credible' ice margin reconstructions from Hughes et al. (2016) are also used to constrain this time period to 17–14 ka.

After the LGM, where ice streams extended to the shelf edge (Ottesen et al., 2005), the western BSIS began to retreat from the shelf edge at ~19–18 ka (Elverhøi et al., 1995; Landvik et al., 1998; Rasmussen et al., 2007). There is uncertainty in how the eastern BSIS retreated due to a lack of published data on- and offshore Novaya Zemlya. In a recent review Patton et al. (2015) showed that ice cover on Novaya Zemlya was confluent with the BSIS at 16 ka. Alternatively, the Hughes et al. (2016) 'most-credible' reconstruction, which is based on geomorphological and geochronological data, suggests the ice covers were separate from at least 17 ka. Hughes et al. (2016) dedicate a detailed discussion to the problems associated with the lack of evidence in the eastern Barents Sea and this study only concentrates on the salient points when appropriate. Since the work presented here is

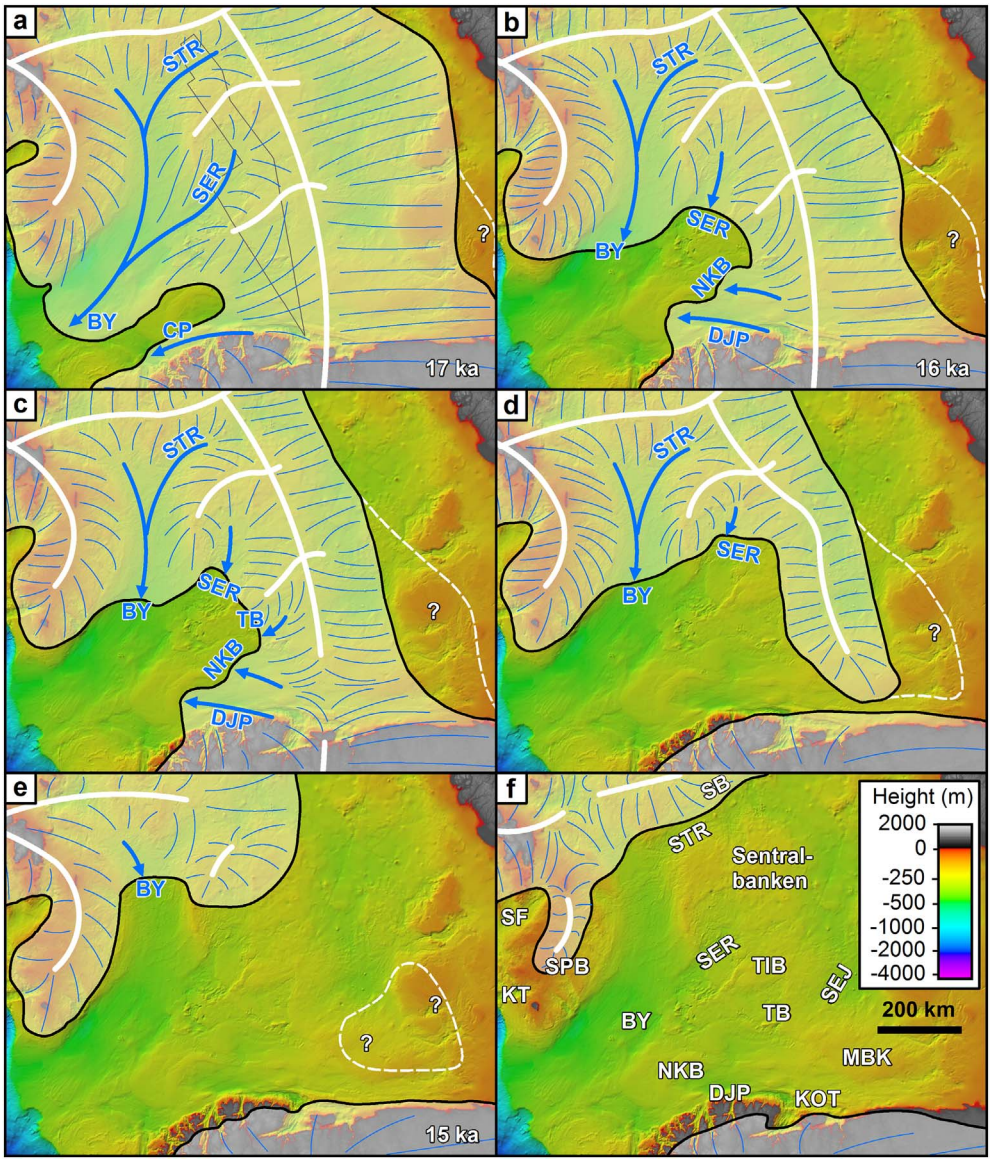

Fig. 11. (a–f) Time-slice reconstruction of the Barents Sea Ice Sheet between 17 and 14 ka. In panels with dates the ice sheet margin is the 'most-credible' reconstruction from Hughes et al. (2016). The ice margins and flow patterns have been generalised from studies discussed in the main text and from this study. White lines indicate possible locations of ice divides, whilst blue arrows and lines indicate ice streams and general flowlines, respectively. These are necessarily schematic due to the limited availability of data and are based on correlations across different sets of geomorphological data. Thus, this reconstruction provides a simplified pattern of retreat after ice streams reduced ice volume in the saddle area before the eventual separation of the Barents Sea Ice Sheet from the Fennoscandian Ice Sheet. The question marks refer to uncertainty in ice margin extent in the southeastern Barents Sea and a proposal for greater ice cover extent in the central and eastern Barents Sea. Abbreviations are the same as Fig. 1 except for coast-parallel ice stream (CP), Murmanskbanken (MBK), and Sentraldjupet (SEJ). See Fig. 2 for location. (For interpretation of the references to colour in this figure legend, the reader is referred to the web version of this article.)

designed to add more detail to the reconstructions of Hughes et al. (2016), their interpretation that Novaya Zemlya was separated from the BSIS at 17 ka is followed.

From 17 to 16 ka (Fig. 11a and b) several ice streams are thought to have been active in the central Barents Sea, including the Bjørnøyrenna Ice Stream, which retreated through the trough episodically (Rüther et al., 2012; Bjarnadóttir et al., 2014). At 17 ka, a coast-parallel ice stream is thought to have been active along the north Norwegian coastline (Ottesen et al., 2008b; Winsborrow et al., 2010). Evidence of ice streaming in Sentralbankrenna (Fig. 4a) suggests an ice stream here was probably a tributary of the Bjørnøyrenna Ice Stream, which was temporarily stable at the GZW in outer Bjørnøyrenna (Winsborrow et al., 2010; Rüther et al., 2011). Ice streaming in Sentralbankrenna and Storbankrenna is partly facilitated by the location of an ice divide on the bank areas that causes convergence of ice into the troughs (Fig. 11a). At 16 ka (Fig. 11b) the reconstruction from Hughes et al. (2016) shows that the Bjørnøyrenna Ice Stream retreated through the trough to a second ice margin observed by Winsborrow et al. (2010). Using the 'stage 3' reconstruction from Winsborrow et al. (2010) to populate the ice margin with flow characteristics, the margins of the Nordkappbanken-east and Djuprenna ice streams were stable offshore northern Norway (Fig. 11b). During this period it is plausible that fringing ice shelves may have occupied the cavity that was created by the retreat of the Bjørnøyrenna, Sentralbankrenna, and mainland Norwegian ice to the northeast, east, and southeast respectively. The presence of ice shelves and a dense mélange of calved icebergs and sea ice may have provided an important buttress that stabilised the margin, e.g. Scambos et al. (2004) and Amundson et al. (2010). Thus, fringing ice shelves might account for the stillstand deposits that are observed offshore in this area. Smaller troughs off of Svalbard and Spitsbergbanken, such as Kveithola and Storfjorden, have also shown similar episodic retreat (Pedrosa et al., 2011; Bjarnadóttir et al., 2013; Llopart et al., 2015).

After 16 ka (Fig. 11c), further retreat of the Bjørnøyrenna Ice Stream

Table 1
Descriptions and references of flow-sets used to reconstruct ice sheet evolution in the central Barents Sea.

Flow-set	Description	Reference(s)
1	The trough of Storbankrenna is interpreted to have been occupied by fast-flowing ice that fed into the main trunk of the Bjørnøyrenna Ice Stream, most likely at the LGM.	Ottesen et al. (2005); Bjarnadóttir et al. (2014); This study
2	Evidence from MSGLs suggesting evidence for the Nordkappbanken-east Ice Stream.	Winsborrow et al. (2010)
3	MSGLs, GZW, and acoustic data indicate the presence of an ice stream in Sentralbankrenna that was temporarily stable at GZW-1.	Bjarnadóttir et al. (2014); This study
4	Sporadic observation of MSGLs suggesting fast-flowing ice in the area of Tiddlybanken.	Bjarnadóttir et al. (2014); This study
5	MSGLs and GZW-2 show the further retreat and temporary stillstand of an ice stream in Sentralbankrenna.	This study
6	Sediment ridges interpreted as ice margin positions on the southwestern area of Sentralbanken.	Bjarnadóttir et al. (2014)
7	MSGLs and GZW-3 show the further retreat and temporary stillstand of an ice stream in Sentralbankrenna.	This study
8	Moraine ridge suggesting the presence of a temporary stillstand on Murmanskbanken.	Svendsen et al. (2004); Bjarnadóttir et al. (2014);
9	Moraine ridge indicating ice sheet margin of ice flowing from Storbanken.	This study
10	MSGLs superimposed on flow-set 9. Several large moraines and retreat moraines indicate slow retreat of the ice margin in Storbankrenna.	This study
11	CSRs indicate the rapid lift off of a stagnant ice margin. Small retreat (possibly annual) moraines then indicate progressive retreat of the ice margin to the northeast.	This study
12	GZW-4 indicates ice mass thinning and floatation of the ice cover as it retreated north-northeastward onto Storbanken.	This study

and the Nordkappbanken-east and Djuprenna ice streams led to an increase in the size of the ice free area. The retreat of the ice stream in Sentralbankrenna to GZW-1 is correlated with ice margin number two in Bjørnøyrenna from Bjarnadóttir et al. (2014). The locations of the ice divides across the bank areas are still driving the convergence of ice in Storbankrenna and Sentralbankrenna to aid fast ice flow. The ice margin positions of the Nordkappbanken-east and Djuprenna ice streams are thought to still be same as the previous time-slice, but with the addition of topographically-driven ice streaming from Tiddlybanken (Fig. 4e). The loss of any buttressing in the central Barents Sea may have provided the catalyst for reducing backstresses and allowing the ice stream flowing from Tiddlybanken to have been activated. Several ice streams are now operating in the central Barents Sea, in particular in the area of the ice sheet saddle. The combined mass loss by the ice streams would have drawn down the ice saddle over the southern part of the central Barents Sea at this time.

In time-slice 4 (Fig. 11d), the FIS is thought to have uncoupled from the BSIS in the region of the Djuprenna and Kola Troughs offshore Northern Norway where deeper water depths may have exacerbated mass loss and eventual uncoupling. This uncoupling is partially supported by the onshore radial pattern of ice margin retreat that is parallel to the coastline of the Kola Peninsula (Hättestrand and Clark, 2006; Hughes et al., 2016; Stroeven et al., 2016). Observations of moraines on Murmanskbanken indicate ice flow from the east (Svendsen et al., 2004; Bjarnadóttir et al., 2014), suggesting the ice divide may have moved eastward in the central Barents Sea. In this time-slice (Fig. 11d) and those preceding, it is proposed that a larger ice extent in the southeastern Barents Sea may have been a pre-requisite for an ice divide to remain for a sufficiently long enough time to form the Murmanskbanken moraines. As the Bjørnøyrenna Ice Stream episodically retreated through the trough, the ice margin stabilised at position three from Bjarnadóttir et al. (2014) and this is tentatively correlated to GZW-2 in Sentralbankrenna. In the intra-ice stream area between Bjørnøyrenna and Sentralbankrenna, a number of retreat moraines (Bjarnadóttir et al., 2014) indicate slow retreat of the ice margin onto Sentralbanken.

At 15 ka (Fig. 11e) the central Barents Sea was almost fully deglaciated with marine sedimentation suggested at, or shortly after this time, in the western and central Barents Sea (Polyak et al., 1995; Rüther et al., 2012), showing the gradual degradation of the marine-based ice sheet. Offshore ice is thought to have only been present on Storbanken, Spitsbergenbanken, and Sentralbanken. However, it is proposed that an ice cover over Murmanskbanken may still have been present as a discrete entity, as its margins slowly retreated to the higher topography of the bank. After the demise of the Sentralbankrenna Ice Stream, the ice cover over Sentralbanken likely began a similar, gradual retreat after the deposition of GZW-3. The Bjørnøyrenna Ice Stream appears to have still been active during the late glacial (Bjarnadóttir et al., 2014).

In the final time-slice (Fig. 11f), a major reorganisation of the remaining ice sheet is proposed, with fragmentation of the ice divides inferred to be a necessity to account for observations of ice flow on or near Storbanken (Hogan et al., 2010; Bjarnadóttir et al., 2014). Ice margin position nine for the Bjørnøyrenna Ice Stream from Bjarnadóttir et al. (2014) is proposed to correlate with GZW-4 from this study. The outermost part of Spitsbergenbanken is completely deglaciated after the Kveithola trough became ice-free at ~14.2 ka (Rüther et al., 2012), whilst a local ice divide is used to infer a radial retreat pattern that can account for moraines observed on the bank (Rüther et al., 2012).

It seems likely that with the vastly reduced extent of the ice sheet that if the Bjørnøyrenna Ice Stream remained active, it was only so for a short period of time. Ice sheet flow is thought to have been to the south of Kong Karls Land toward Bjørnøyrenna (Andreassen et al., 2014; Bjarnadóttir et al., 2014), and to the north into the Kvitøya and Franz Victoria troughs (Hogan et al., 2010; Batchelor et al., 2011). This flow could have, much like during the initial separation from the FIS, drawn-down ice volume sufficiently to separate the ice cover on Svalbard with that over Storbanken. Coeval with this drawdown, it is postulated that the ice cover on Spitsbergenbanken was close to separating from the ice cover on Svalbard. This reconstruction would account for the ice margin positions on the south western part of Storbanken observed by Bjarnadóttir et al. (2014) and the reconstruction on Spitsbergbanken described above when the ice masses separated during the Late Bølling/Early Allerød (14.2–13.9 cal. ka BP) (Rüther et al., 2012).

Through the deglaciation, the dynamic drawdown of ice masses by ice streaming meant that topographic control and retreat of grounding-lines to shallower water depths became a controlling factor on ice sheet flow patterns and the location of ice divides. As has been discussed above, the seafloor record in the western and northern Barents Sea has been well-studied, and multiple observations of ice flow and margin positions have been constrained with a limited amount of geochronological data (Ottesen et al., 2005, 2008b; Dowdeswell et al., 2010; Hogan et al., 2010; Winsborrow et al., 2010, 2011; Batchelor et al., 2011; Rüther et al., 2012; Bjarnadóttir et al., 2013, 2014; Andreassen et al., 2014). In the eastern Barents and Kara Seas our understanding is, by comparison, relatively poor (Hughes et al., 2016).

This paper concentrates on the key point that there is great deal of uncertainty in the timing of (de)glaciation and the characteristics of the ice cover on Novaya Zemlya. The post-glacial rebound of Novaya Zemlya of ~15 m, dated to ~7 ka BP (Zeeberg et al., 2001) is in major

contrast to the rebound of ~100 m observed from raised beaches on Kong Karls Land (Forman et al., 1995). Zeeberg et al. (2001) suggest that a thin ice sheet over Novaya Zemlya may have prevailed though the deglaciation until the Holocene. However, in the reconstructions of Hughes et al. (2016), and thus the regional model of deglaciation refined in this paper, Novaya Zemlya was deglaciated as early as 18 ka. This is supported by ^{14}C dates collected from the west coast of Novaya Zemlya (Forman et al., 1999) and the limited postglacial marine limit on Novaya Zemlya. As to why Novaya Zemlya deglaciated much earlier than elsewhere in the Barents Sea might be explained by precipitation starvation and an ensuing negative mass balance. The current lack of geomorphological data offshore Novaya Zemlya increases this uncertainty on the demise of the eastern BSIS.

This framework builds on the observations of Hughes et al. (2016) and aims to provide a reconstruction of ice sheet evolution during an important period of ice sheet separation in the Barents Sea. Although the synthesis presented here (Fig. 11) is fitted to all currently available landform records and timescales, the uncertainties in the eastern Barents Sea mean that as more geological, geophysical, and geochronological data become available, this reconstruction can be tested, challenged, and modified. This model can be used as a basis for developing a more complete model of how the marine-based glaciation of the Barents Sea evolved after the LGM.

5.3. Implications for marine-based glaciation

During BSIS deglaciation, ice stream activity led to the gradual drawdown and collapse of the ice saddle joining the BSIS and FIS (Fig. 11). After separation of the two ice sheets, the FIS retreated onshore (Hughes et al., 2016; Stroeven et al., 2016), whilst the BSIS remained largely marine-based. Ice saddle collapses in North America and in the North Sea have been shown to drive mass loss through increased ice stream calving (Gregoire et al., 2012; Sejrup et al., 2016) and this was likely the dominant process leading separation in the central Barents Sea.

In the central Barents Sea and Bjørnøyrenna, retreating ice margins have been shown to cycle through phases of retreat, advance, and stagnation (Bjarnadóttir et al., 2014). Variability in mass balance through the deglaciation would have changed ice sheet geometry, such that frequent reorganisation of ice domes and ice divides (as described in the previous section) could have caused a direct response in ice sheet dynamics, locations of ice streams, and meltwater distribution (Bjarnadóttir et al., 2014; Piasecka et al., 2016). During deglaciation the geomorphological record in the central Barents Sea suggests that fast-flowing ice was primarily restricted to the Bjørnøyrenna, Storbankrenna, and Sentralbankrenna troughs (Fig. 11). Routing of ice streams in topographically low areas would have resulted in an increased negative mass balance as more ice was brought below the equilibrium line altitude. With rising temperatures and sea level, it might be expected that retreat of the ice margin would have accelerated. However, this is not the case and the geomorphological record suggests that after saddle collapse retreat of the margin was episodic, not rapid.

Although more geological and geochronological observations are required to validate the proposed reconstructions, this work shows that through time, the bank areas were likely modulating spatio-temporal changes in the locations of ice domes, ice divides and ice streaming (Fig. 11). As ice streams and temperature rise continued to enforce a negative mass balance, it is proposed that a number of these ice domes prevailed until they fragmented during the final demise of the BSIS with separate domes present on mainland Svalbard and Storbanken. This interpretation honours ice margin positions observed across the central Barents Sea (Svendsen et al., 2004; Bjarnadóttir et al., 2014).

Migration of the BSIS ice divides (Fig. 11) is important because recent observations from the WAIS suggest that the Western Divide, which separates ice flowing into the Weddell and Ross Seas, has migrated in response to changes in ice sheet dynamics and mass loss (Conway and Rasmussen, 2009). Thus, the behaviour of the BSIS might provide insight into the future evolution of the Western Divide. For example, how the underlying topography might reorganise not just the exact pathways of ice streams but also the volume percentage of ice that they drain, once the ice divide has migrated.

Although the exact geological setting of the WAIS is different to the BSIS, observations discussed here and elsewhere in the Barents Sea (Winsborrow et al., 2010, 2011; Andreassen et al., 2014; Bjarnadóttir et al., 2014) have shown changes in ice sheet dynamics that are potentially comparable to those observed on contemporary WAIS ice streams (Joughin and Tulaczyk, 2002; Anandakrishnan et al., 2007; Hulbe and Fahnestock, 2007). Bjarnadóttir et al. (2014) suggest that the cyclicity of changes in ice stream stagnation, flow-switching, and reactivation in the Barents Sea could be attributed to meltwater availability, drainage capabilities of the subsurface, and the effect of buttressing. Similar observations in Antarctica have been observed from palaeo-ice streams and after the collapse of the Larsen B ice shelf (Scambos et al., 2004; Hulbe and Fahnestock, 2007; Bell, 2008). Thus, new insights on the marine-based glaciation of the Barents Sea (such as that presented here) will provide a better understanding of how the WAIS might evolve in the future, especially if meltwater production increases as the climate warms.

6. Conclusions

Observations from new bathymetric data in the central Barents Sea have been integrated with those already published to establish the late Weichselian ice sheet history of the central Barents Sea between 17–14 ka. During this period the BSIS and FIS are thought to have separated (Hughes et al., 2016; Stroeven et al., 2016) and the geomorphological record presented here suggests that the two ice sheets uncoupled in the southern Barents Sea, close to the Djuprenna and Kola troughs. Intense ice streaming is proposed to have led to the rapid drawdown of the ice cover in the saddle area, resulting in a lowering of its ice profile, before the saddle finally collapsed and the two ice sheets uncoupled. As the BSIS retreated through the survey area, the results presented here and in adjacent areas (e.g. Bjarnadóttir et al., 2014) show that retreat in the central Barents Sea was punctuated by periods of stillstand and advance. These changes are interpreted to have been in response to changes in ice dynamics that were becoming increasingly controlled by the seafloor topography as the grounding-line retreated to shallower water depths. Importantly, punctuation of ice margin retreat implies that after the saddle collapsed the BSIS did not rapidly destabilise or disintegrate.

Although a chronology of events in accordance with other studies in the region has been assumed, the chronology is tentative. With future geochronological data for ice-free conditions, the pattern of retreat described here can be refined and tested. Additional geophysical mapping of the seafloor and acoustic stratigraphy are crucial and may result in the reinterpretation of the seafloor features. This is especially the case to the east and north of the survey where a number of the landforms terminate at the boundaries of the data and are not well-represented in regional, lower-resolution bathymetry data. Developing more detailed reconstructions for the demise of the BSIS, such as that presented here, is essential for developing a more complete model of marine-based glaciation and may provide insights into how the WAIS might evolve under a warming climate.

Acknowledgments

This work was supported by the Natural Environment Research Council (NERC grant reference number NE/K500859/1) and Cairn Energy who jointly funded AMWN. Schlumberger and ESRI are thanked for providing Petrel and Arc software. We would like to thank the MAREANO Programme for providing the multibeam data used in this study (available at www.mareano.no) and Arnstein Osvik for helping us

to acquire the data. We also thank Simon H. Brocklehurst, Matthew Warke, the editor, and three reviewers for very detailed comments that significantly improved the initial manuscript.

References

Amundson, J.M., Fahnestock, M., Truffer, M., Brown, J., Lüthi, M.P., Motyka, R.J., 2010. Ice mélange dynamics and implications for terminus stability, Jakobshavn Isbræ, Greenland. J. Geophys. Res. Earth Surf. 115, F01005.

Anandakrishnan, S., Cartania, G., Alley, R.B., Horgan, H.J., 2007. Discovery of till deposition at the grounding line of Whillans Ice Stream. Science 315, 1835–1838.

Andreassen, K., Winsborrow, M., 2009. Signature of ice streaming in Bjørnøyrenna, Polar North Atlantic, through the Pleistocene and implications for ice-stream dynamics. Ann. Glaciol. 50, 17–26.

Andreassen, K., Nilssen, E.G., Ødegaard, C.M., 2007. Analysis of shallow gas and fluid migration within the Plio-Pleistocene sedimentary succession of the SW Barents Sea continental margin using 3D seismic data. Geo-Mar. Lett. 27, 155–171.

Andreassen, K., Winsborrow, M.C.M., Bjarnadóttir, L.R., Rüther, D.C., 2014. Ice stream retreat dynamics inferred from an assemblage of landforms in the northern Barents Sea. Quat. Sci. Rev. 92, 246–257.

Banerjee, I., McDonald, B.C., 1975. Nature of esker sedimentation. In: Jopling, A.V., McDonald, B.C. (Eds.), Glaciofluvial and Glaciolacustrine Sedimentation. SEPM, Oklahoma, pp. 132–154.

Bass, D.W., Woodworth-Lynas, C.M.T., 1988. Iceberg crater marks on the sea floor, Labrador shelf. Mar. Geol. 79, 243–260.

Batchelor, C.L., Dowdeswell, J.A., 2015. Ice-sheet grounding-zone wedges (GZWs) on high-latitude continental margins. Mar. Geol. 363, 65–92.

Batchelor, C.L., Dowdeswell, J.A., Hogan, K.A., 2011. Late Quaternary ice flow and sediment delivery through Hinlopen Trough, Northern Svalbard margin: Submarine landforms and depositional fan. Mar. Geol. 284, 13–27.

Bell, R.E., 2008. The role of subglacial water in ice-sheet mass balance. Nat. Geosci. 1, 297–304.

Bennett, M.R., 2003. Ice streams as the arteries of an ice sheet: their mechanics, stability and significance. Earth Sci. Rev. 61, 309–339.

Bentley, M.J., Ó Cofaigh, C., Anderson, J.B., Conway, H., Davies, B., Graham, A.G.C., Hillenbrand, C.-D., Hodgson, D.A., Jamieson, S.S.R., Larter, R.D., Mackintosh, A., Smith, J.A., Verleyen, E., Ackert, R.P., Bart, P.J., Berg, S., Brunstein, D., Canals, M., Colhoun, E.A., Crosta, X., Dickens, W.A., Domack, E., Dowdeswell, J.A., Dunbar, R., Ehrmann, W., Evans, J., Favier, V., Fink, D., Fogwill, C.J., Glasser, N.F., Gohl, K., Golledge, N.R., Goodwin, I., Gore, D.B., Greenwood, S.L., Hall, B.L., Hall, K., Hedding, D.W., Hein, A.S., Hocking, E.P., Jakobsson, M., Johnson, J.S., Jomelli, V., Jones, R.S., Klages, J.P., Kristoffersen, Y., Kuhn, G., Leventer, A., Licht, K., Lilly, K., Lindow, J., Livingstone, S.J., Massé, G., McGlone, M.S., McKay, R.M., Melles, M., Miura, H., Mulvaney, R., Nel, W., Nitsche, F.O., O'Brien, P.E., Post, A.L., Roberts, S.J., Saunders, K.M., Selkirk, P.M., Simms, A.R., Spiegel, C., Stolldorf, T.D., Sugden, D.E., van der Putten, N., van Ommen, T., Verfaillie, D., Vyverman, W., Wagner, B., White, D.A., Witus, A.E., Zwartz, D., 2014. A community-based geological reconstruction of Antarctic Ice Sheet deglaciation since the Last Glacial Maximum. Quat. Sci. Rev. 100, 1–9.

Bjarnadóttir, L.R., Rüther, D.C., Winsborrow, M.C.M., Andreassen, K., 2013. Grounding-line dynamics during the last deglaciation of Kveithola, W Barents Sea, as revealed by seabed geomorphology and shallow seismic stratigraphy. Boreas 42, 84–107.

Bjarnadóttir, L.R., Winsborrow, M.C.M., Andreassen, K., 2014. Deglaciation of the central Barents Sea. Quat. Sci. Rev. 92, 208–226.

Bondevik, S., Mangerud, J., Ronnert, L., Salvigsen, O., 1995. Postglacial sea-level history of Edgeøya and Barentsøya, eastern Svalbard. Polar Res. 14, 153–180.

Boulton, G.S., 1986. Push-moraines and glacier-contact fans in marine and terrestrial environments. Sedimentology 33, 677–698.

Boulton, G.S., Clark, C.D., 1990. A highly mobile Laurentide ice sheet revealed by satellite images of glacial lineations. Nature 346, 813–817.

Brown, C.S., Newton, A.M.W., Huuse, M., Buckley, F., 2017. Iceberg scours, pits, and pockmarks in the North Falkland Basin. Mar. Geol. 386, 140–152.

Butt, F.A., Elverhøi, A., Solheim, A., Forsberg, C.F., 2000. Deciphering Late Cenozoic development of the western Svalbard Margin from ODP Site 986 results. Mar. Geol. 169, 373–390.

Clark, C.D., 1993. Mega-scale glacial lineations and cross-cutting ice-flow landforms. Earth Surf. Process. Landf. 18, 1–29.

Clark, C.D., 1997. Reconstructing the evolutionary dynamics of former ice sheets using multi-temporal evidence, remote sensing and GIS. Quat. Sci. Rev. 16, 1067–1092.

Clark, C.D., Tulaczyk, S.M., Stokes, C.R., Canals, M., 2003. A groove-ploughing theory for the production of mega-scale glacial lineations, and implications for ice-stream mechanics. J. Glaciol. 49, 240–256.

Clark, C.D., Hughes, A.L.C., Greenwood, S.L., Jordan, C., Sejrup, H.P., 2012. Pattern and timing of retreat of the last British-Irish Ice Sheet. Quat. Sci. Rev. 44, 112–146.

Conway, H., Rasmussen, L.A., 2009. Recent thinning and migration of the Western Divide, central West Antarctica. Geophys. Res. Lett. 36, L12502.

Denton, G.H., Anderson, R.F., Toggweiler, J.R., Edwards, R.L., Schaefer, J.M., Putnam, A.E., 2010. The Last Glacial termination. Science 328, 1652–1656.

Dowdeswell, J.A., Fugelli, E.M.G., 2012. The seismic architecture and geometry of grounding-zone wedges formed at the marine margins of past ice sheets. Geol. Soc. Am. Bull. 124, 1750–1761.

Dowdeswell, J.A., Ottesen, D., Evans, J., Ó Cofaigh, C., Anderson, J.B., 2008. Submarine glacial landforms and rates of ice-stream collapse. Geology 36, 819–822.

Dowdeswell, J.A., Hogan, K.A., Evans, J., Noormets, R., Ó Cofaigh, C., Ottesen, D., 2010. Past ice-sheet flow east of Svalbard inferred from streamlined subglacial landforms. Geology 38, 163–166.

Dowdeswell, J.A., Canals, M., Jakobsson, M., Todd, B.J., Dowdeswell, E.K., Hogan, K.A., 2016. Atlas of Submarine Glacial Landforms: Modern, Quaternary and Ancient, Memoirs. Geological Society, London.

Elverhøi, A., Solheim, A., 1983. The Barents Sea ice sheet - a sedimentological discussion. Polar Res. 1, 23–42.

Elverhøi, A., Andersen, E.S., Dokken, T., Hebbeln, D., Spielhagen, R., Svendsen, J.I., Sørflaten, M., Rørnes, A., Hald, M., Forsberg, C.F., 1995. The growth and decay of the Late Weichselian ice sheet in western Svalbard and adjacent areas based on provenance studies of marine sediments. Quat. Res. 44, 303–316.

Engelhardt, H., Kamb, B., 1997. Basal hydraulic system of a West Antarctic ice stream: constraints from borehole observations. J. Glaciol. 43, 207–230.

Evans, D.J.A., Rea, B.R., 1999. Geomorphology and sedimentology of surging glaciers: a land-systems approach. Ann. Glaciol. 28, 75–82.

Faleide, J.I., Vågnes, E., Gudlaugsson, S.T., 1993. Late Mesozoic– Cenozoic evolution of the southwestern Barents Sea in a regional rift-shear tectonic setting. Mar. Pet. Geol. 10, 186–214.

Faleide, J.I., Solheim, A., Fiedler, A., Hjelstuen, B.O., Andersen, E.S., Vanneste, K., 1996. Late Cenozoic evolution of the western Barents SeaeSvalbard continental margin. Glob. Planet. Chang. 12, 53–74.

Faleide, J.I., Bjørlykke, K., Gabrielsen, R.H., 2010. Geology of the Norwegian Continental Shelf. In: Bjørlykke, K. (Ed.), Petroleum Geoscience: From Sedimentary Environments to Rock Physics. Springer, Berlin, pp. 467–499.

Fiedler, A., Faleide, J.I., 1996. Cenozoic sedimentation along the southwestern Barents Sea margin in relation to uplift and erosion of the shelf. Glob. Planet. Chang. 12, 75–93.

Flink, A.E., Noormets, R., Kirchner, N., Benn, D.I., Luckman, A., Lovell, H., 2015. The evolution of a submarine landform record following recent and multiple surges of Tunabreen glacier, Svalbard. Quat. Sci. Rev. 108, 37–50.

Forman, S.L., Lubinski, D., Miller, G.H., Snyder, J., Matishov, G., Korsun, S., Myslivets, V., 1995. Postglacial emergence and distribution of late Weichselian ice-sheet loads in the northern Barents and Kara seas, Russia. Geology 23, 113–116.

Forman, S.L., Lubinski, D.J., Zeeberg, J.J., Polyak, L., Miller, G.H., Matishov, G., Tarasov, G., 1999. Postglacial emergence and Late Quaternary glaciation on northern Novaya Zemlya, Arctic Russia. Boreas 28, 133–145.

Gabrielsen, V., Færseth, R.B., Jensen, L.N., Kalheim, J.E., Riis, F., 1990. Structural elements of the Norwegian continental shelf. Part I: The Barents Sea Region. Norw. Petrol. Direct. Bull. 6.

Gernigon, L., Brönner, M., Roberts, D., Olesen, O., Nasuti, A., Yamasaki, T., 2014. Crustal and basin evolution of the southwestern Barents Sea: From Caledonian orogeny to continental breakup. Tectonics 33, 347–373.

Graham, A.G.C., Dutrieux, P., Vaughan, D.G., Nitsche, F.O., Gyllencreutz, R., Greenwood, S.L., Larter, R.D., Jenkins, A., 2013. Seabed corrugations beneath an Antarctic ice shelf revealed by autonomous underwater vehicle survey: Origin and implications for the history of Pine Island Glacier. J. Geophys. Res. Earth Surf. 118, 1356–1366.

Greenwood, S.L., Clark, C.D., 2009. Reconstructing the last Irish Ice Sheet 1: changing flow geometries and ice flow dynamics deciphered from the glacial landform record. Quat. Sci. Rev. 28, 3085–3100.

Gregoire, L.J., Payne, A.J., Valdes, P.J., 2012. Deglacial rapid sea level rises caused by ice-sheet saddle collapses. Nature 487, 219–222.

Hättestrand, C., Clark, C.D., 2006. The glacial geomorphology of Kola Peninsula and adjacent areas in the Murmansk Region, Russia. J. Maps 2, 30–42.

Henderson, P.J., 1988. Sedimentation in an esker system influenced by bedrock topography near Kingston, Ontario. Can. J. Earth Sci. 25, 987–999.

Hogan, K.A., Dowdeswell, J.A., Noormets, R., Evans, J., Ó Cofaigh, C., 2010. Evidence for full-glacial flow and retreat of the Late Weichselian Ice Sheet from the waters around Kong Karls Land, eastern Svalbard. Quat. Sci. Rev. 29, 3563–3582.

Hughes, T.J., 1981. The weak underbelly of the West Antarctic Ice Sheet. J. Glaciol. 27, 518–525.

Hughes, A.L.C., Clark, C.D., Jordan, C.J., 2014. Flow-pattern evolution of the last British Ice Sheet. Quat. Sci. Rev. 89, 148–168.

Hughes, A.L.C., Gyllencreutz, R., Lohne, Ø.S., Mangerud, J., Svendsen, J.I., 2016. The last Eurasian ice sheets – a chronological database and time-slice reconstruction, DATED-1. Boreas 45, 1–45.

Hulbe, C., Fahnestock, M., 2007. Century-scale discharge stagnation and reactivation of the Ross ice streams, West Antarctica. J. Geophys. Res. 112, F03S27.

Huuse, M., Lykke-Andersen, H., 2000. Overdeepened Quaternary valleys in the eastern Danish North Sea: morphology and origin. Quat. Sci. Rev. 19, 1233–1253.

Ingólfsson, Ó., Landvik, J.Y., 2013. The Svalbard-Barents Sea ice-sheet - Historical, current and future perspectives. Quat. Sci. Rev. 64, 33–60.

Jakobsson, M., Anderson, J.B., Nitsche, F.O., Dowdeswell, J.A., Gyllencreutz, R., Kirchner, N., Mohammad, R., O'Regan, M., Alley, R.B., Anandakrishnan, S., Eriksson, B., Kirshner, A.E., Fernandez, R., Stolldorf, T., Minzoni, R., Majewski, W., 2011. Geological record of ice shelf break-up and grounding line retreat, Pine Island Bay, West Antarctica. Geology 39, 691–694.

Jakobsson, M., Andersen, J.B., Nitsche, F.O., Gyllencreutz, R., Kirshner, A.E., Kirchner, N., O'Regan, M., Mohammad, R., Eriksson, B., 2012a. Ice sheet retreat dynamics inferred from glacial morphology of the central Pine Island Bay Trough, West Antarctica. Quat. Sci. Rev. 38, 1–10.

Jakobsson, M., Mayer, L., Coakley, B., Dowdeswell, J.A., Forbes, S., Fridman, B., Hodnesdal, H., Noormets, R., Pedersen, R., Rebesco, M., Schenke, H.W., Zarayskaya, Y., Accettella, D., Armstrong, A., Anderson, R.M., Bienhoff, P., Camerlenghi, A., Church, I.M.E., Gardner, J.V., Hall, J.K., Hell, B., Hestvik, O., Kristoffersen, Y., Marcussen, C., Mohammad, R., Mosher, D., Nghiem, S.V., Pedrosa, M.T., Travaglini, P.G., Weatherall, P., 2012b. The International Bathymetric Chart of the Arctic Ocean

(IBCAO) Version 3.0. Geophys. Res. Lett. 39, L12609.
Jakobsson, M., Andreassen, K., Bjarnadóttir, L.R., Dove, D., Dowdeswell, J.A., England, J.H., Funder, S., Hogan, K., Ingólfsson, Ó., Jennings, A., Larsen, N.K., Kirchner, N., Landvik, J.Y., Mayer, L., Mikkelsen, N., Möller, P., Niessen, F., Nilsson, J., O'Regan, M., Polyak, L., Nørgaard-Pedersen, N., Stein, R., 2014. Arctic Ocean glacial history. Quat. Sci. Rev. 92, 40–67.
Jamieson, S.S.R., Vieli, A., Livingstone, S.J., Ó Cofaigh, C., Stokes, C., Hillenbrand, C.-D., Dowdeswell, J.A., 2012. Ice-stream stability on a reverse bed slope. Nat. Geosci. 5, 799–802.
Jansen, E., Sjøholm, J., 1991. Reconstruction of glaciations over the past 6 Myr from ice born deposits in the Norwegian Sea. Nature 349, 600–603.
Jessen, S.P., Rasmussen, T.L., Nielsen, T., Solheim, A., 2010. A new Late Weichselian and Holocene marine chronology for the western Svalbard slope 30,000-0 cal years BP. Quat. Sci. Rev. 29, 1301–1312.
Joughin, I., Alley, R.B., 2011. Stability of the West Antarctic ice sheet in a warming world. Nat. Geosci. 4, 506–513.
Joughin, I., Tulaczyk, S., 2002. Positive mass balance of the Ross Ice Streams, West Antarctica. Science 295, 476–480.
Junttila, J., Aagaard-Sørensen, S., Husum, K., Hald, M., 2010. Late Glacial-Holocene clay minerals elucidating glacial history in the SW Barents Sea. Mar. Geol. 276, 71–85.
Kleman, J., Borgström, I., 1996. Reconstruction of palaeo-ice sheets: the use of geomorphological data. Earth Surf. Process. Landf. 21, 893–909.
Kleman, J., Hättestrand, C., Stroeven, A.P., Jansson, K.N., De Angelis, H., Borgström, I., 2006. Reconstruction of palaeo-ice sheets - Inversion of their glacial geomorphological record. In: Knight, J. (Ed.), Glacier Science and Environmental Change. Blackwell Publishing, Oxford, pp. 192–198.
Knies, J., Matthiessen, J., Vogt, C., Laberg, J.S., Hjelstuen, B.O., Smelror, M., Larsen, E., Andreassen, K., Eidvin, T., Vorren, T.O., 2009. The Plio-Pleistocene glaciation of the Barents Sea–Svalbard region: a new model based on revised chronostratigraphy. Quat. Sci. Rev. 28, 812–829.
Kyrke-Smith, T.M., Katz, R.F., Fowler, A.C., 2013. Subglacial hydrology and the formation of ice streams. Proc. R. Soc. Lond. A 470, 20130494.
Laberg, J.S., Vorren, T.O., 1996. The Middle and Late Pleistocene evolution of the Bear Island Trough Mouth Fan. Glob. Planet. Chang. 12, 309–330.
Laberg, J.S., Andreassen, K., Vorren, T.O., 2011. Late Cenozoic erosion of the high-latitude southwestern Barents Sea shelf revisited. Geol. Soc. Am. Bull. 124, 77–88.
Lambeck, K., Rouby, H., Purcell, A., Sun, Y., Sambridge, M., 2014. Sea level and global ice volumes from the Last Glacial Maximum to the Holocene. Proc. Natl. Acad. Sci. U. S. A. 111, 15296–15303.
Landvik, J.Y., Bondevik, S., Elverhøi, A., Fjeldskaar, W., Mangerud, J., Salvigsen, O., Siegert, M.J., Svendsen, J.I., Vorren, T.O., 1998. The Last Glacial Maximum of Svalbard and the Barents Sea area: ice sheet extent and configuration. Quat. Sci. Rev. 17, 43–75.
Le Brocq, A.M., Ross, N., Griggs, J.A., Bingham, R.G., Corr, H.J.F., Ferraccioli, F., Jenkins, A., Jordan, T.A., Payne, A.J., Rippin, D.M., Siegert, M.J., 2013. Evidence from ice shelves for channelized meltwater flow beneath the Antarctic Ice Sheet. Nat. Geosci. 6, 945–948.
Lindén, M., Möller, P., 2005. Marginal formation of De Geer moraines and their implications to the dynamics of grounding-line recession. J. Quat. Sci. 20, 113–133.
Livingstone, S.J., Utting, D.J., Ruffell, A., Clark, C.D., Pawley, S., Atkinson, N., Fowler, A.C., 2016. Discovery of relict subglacial lakes and their geometry and mechanism of drainage. Nat. Commun. 7, 11767.
Llopart, J., Urgeles, R., Camerlenghi, A., Lucchi, R.G., Rebesco, M., De Mol, B., 2015. Late Quaternary development of the Storfjorden and Kveithola Trough Mouth Fans, northwestern Barents Sea. Quat. Sci. Rev. 129, 68–84.
Mercer, J.H., 1970. A former ice sheet in the Arctic Ocean. Palaeogeogr. Palaeoclimatol. Palaeoecol. 8, 19–27.
Newton, A.M.W., Huuse, M., Brocklehurst, S.H., 2016. Buried iceberg scours reveal reduced North Atlantic Current during the stage 12 deglacial. Nat. Commun. 7, 10927.
Ó Cofaigh, C., 1996. Tunnel valley genesis. Prog. Phys. Geogr. 20, 1–19.
Ottesen, D., Dowdeswell, J.A., 2006. Assemblages of submarine landforms produced by tidewater glaciers in Svalbard. J. Geophys. Res. 111, F01016.
Ottesen, D., Dowdeswell, J.A., Rise, L., 2005. Submarine landforms and the reconstruction of fast-flowing ice streams within a large Quaternary ice sheet: the 2500-km-long Norwegian-Svalbard margin (57°–80°N). Geol. Soc. Am. Bull. 117, 1033–1050.
Ottesen, D., Dowdeswell, J.A., Benn, D.I., Kristensen, L., Christiansen, H.H., Christensen, O., Hansen, L., Lebesbye, E., Forwick, M., Vorren, T.O., 2008a. Submarine landforms characteristic of glacier surges in two Spitsbergen fjords. Quat. Sci. Rev. 27, 1583–1599.
Ottesen, D., Stokes, C.R., Rise, L., Olsen, L., 2008b. Ice-sheet dynamics and ice streaming along the coastal parts of northern Norway. Quat. Sci. Rev. 72, 922–940.
Patton, H., Andreassen, K., Bjarnadóttir, L.R., Dowdeswell, J.A., Winsborrow, M.C.M., Noormets, R., Polyak, L., Auriac, A., Hubbard, A., 2015. Geophysical constraints on the dynamics and retreat of the Barents Sea ice sheet as a paleobenchmark for models of marine ice sheet deglaciation. Rev. Geophys. 53, 1051–1098.
Patton, H., Hubbard, A., Andreassen, K., Winsborrow, M., Stroeven, A.P., 2016. The build-up, configuration, and dynamical sensitivity of the Eurasian ice-sheet complex to Late Weichselian climatic and oceanic forcing. Quat. Sci. Rev. 153, 97–121.
Pedrosa, M.T., Camerlenghi, A., De Mol, B., Urgeles, R., Rebesco, M., Lucchi, R.G., shipboard participants of the SVAIS and EGLACOM Cruises, 2011. Seabed morphology and shallow sedimentary structure of the Storfjorden and Kveithola trough-mouth fans (North West Barents Sea). Mar. Geol. 286, 65–81.
Piasecka, E.D., Winsborrow, M.C.M., Andreassen, K., Stokes, C.R., 2016. Reconstructing the retreat dynamics of the Bjørnøyrenna Ice Stream based on new 3D seismic data from the central Barents Sea. Quat. Sci. Rev. 151, 212–227.
Polyak, L., Lehman, S.J., Gataullin, V., Jull, A.J.T., 1995. Two-step deglaciation of the southeastern Barents Sea. Geology 23, 567–571.
Pritchard, H.D., Arthern, R.J., Vaughan, D.G., Edwards, L.A., 2009. Extensive dynamic thinning on the margins of the Greenland and Antarctic ice sheets. Nature 461, 971–975.
Rasmussen, T.L., Thomsen, E., Ślubowska, M.A., Jessen, S., Solheim, A., Koç, N., 2007. Paleoceanographic evolution of the SW Svalbard margin (76°N) since 20,000 ^{14}C yr BP. Quat. Res. 67, 100–114.
Rignot, E., Casassa, G., Gogineni, P., Krabill, W., Rivera, A., Thomas, R., 2004. Accelerated ice discharge from the Antarctic Peninsula following the collapse of Larsen B ice shelf. Geophys. Res. Lett. 31, L18401.
Rignot, E., Velicogna, I., van den Broeke, M.R., Monaghan, A., Lenaerts, J.T.M., 2011. Acceleration of the contribution of the Greenland and Antarctic ice sheets to sea level rise. Geophys. Res. Lett. 38, L05503.
Rohling, E.J., Grant, K., Bolshaw, M., Roberts, A.P., Siddall, M., Hemleben, C., Kucera, M., 2009. Antarctic temperature and global sea level closely coupled over the past five glacial cycles. Nat. Geosci. 2, 500–504.
Röthlisberger, R., 1972. Water pressure in intra- and sub-glacial channels. J. Glaciol. 11, 177–203.
Rüther, D.C., Mattingsdal, R., Andreassen, K., Forwick, M., Husum, K., 2011. Seismic architecture and sedimentology of a major grounding zone system deposited by the Bjørnøyrenna Ice Stream during Late Weichselian deglaciation. Quat. Sci. Rev. 30, 2776–2792.
Rüther, D.C., Bjarnadóttir, L.R., Junttila, J., Husum, K., Rasmussen, T.L., Lucchi, R.G., Andreassen, K., 2012. Pattern and timing of the northwestern Barents Sea Ice Sheet deglaciation and indications of episodic Holocene deposition. Boreas 41, 494–512.
Ryseth, A., Auguston, J.H., Charnock, M., Haugerud, O., Knutsen, S.M., Midbøe, P.S., Opsahl, J.G., Sundsbøe, G., 2003. Cenozoic stratigraphy and evolution of the Sørvestsnaget Basin, southwestern Barents Sea. Nor. J. Geol. 83, 107–130.
Salvigsen, O., 1981. Radiocarbon dated raised beaches in Kong Karls Land, Svalbard, and their consequences for the glacial history of the Barents Sea area. Geogr. Ann. Ser. B 63, 283–291.
Scambos, T.A., Bohlander, J.A., Shuman, C.A., Skvarca, P., 2004. Glacier acceleration and thinning after ice shelf collapse in the Larsen B embayment, Antarctica. Geophys. Res. Lett. 31, L18402.
Schoof, C., 2007. Ice sheet grounding line dynamics: steady states, stability, and hysteresis. J. Geophys. Res. Earth Surf. 112, F03S28.
Sejrup, H.P., Clark, C.D., Hjelstuen, B.O., 2016. Rapid ice sheet retreat triggered by ice stream debuttressing: Evidence from the North Sea. Geology 44, 355–358.
Shreve, R.L., 1985. Esker characteristics in terms of glacier physics, Katahdin esker system, Maine. Geol. Soc. Am. Bull. 96, 639–646.
Solheim, A., Kristoffersen, Y., 1984. Physical environment Western Barents Sea, 1: 1,500,000: sediments above the upper regional unconformity: thickness, seismic stratigraphy and outline of the glacial history. Nor. Polarinst. Skr. 179B, 3–26.
Solheim, A., Russwurm, L., Elverhøi, A., Berg, M.N., 1990. Glacial geomorphic features in the northern Barents Sea: direct evidence for grounded ice and implications for the pattern of deglaciation and late glacial sedimentation. In: Dowdeswell, J.A., Scourse, J.D. (Eds.), Glacimarine Environments: Processes and Sediments. Geological Society of London, London, pp. 253–268.
Solheim, A., Andersen, E.S., Elverhøi, A., Fiedler, A., 1996. Late Cenozoic depositional history of the western Svalbard continental shelf, controlled by subsidence and climate. Glob. Planet. Chang. 12, 135–148.
Spagnolo, M., Clark, C.D., Ely, J.C., Stokes, C.R., Anderson, J.B., Andreassen, K., Graham, A.G.C., King, E.C., 2014. Size, shape and spatial arrangement of mega-scale glacial lineations from a large and diverse dataset. Earth Surf. Process. Landf. 39, 1432–1448.
Stokes, C.R., Clark, C.D., 1999. Geomorphological criteria for identifying Pleistocene ice streams. Ann. Glaciol. 28, 67–74.
Stokes, C.R., Clark, C.D., 2001. Palaeo-ice streams. Quat. Sci. Rev. 20, 1437–1457.
Stokes, C.R., Corner, G.D., Winsborrow, M.C.M., Husum, K., Andreassen, K., 2014. Asynchronous response of marine-terminating outlet glaciers during deglaciation of the Fennoscandian Ice Sheet. Geology 42, 455–458.
Storrar, R.D., Stokes, C.R., Evans, D.J.A., 2014. Morphometry and pattern of a large sample (> 20,000) of Canadian eskers and implications for subglacial drainage beneath ice sheets. Quat. Sci. Rev. 105, 1–25.
Stroeven, A.P., Hättestrand, C., Kleman, J., Heyman, J., Fabel, D., Fredin, O., Goodfellow, B.W., Harbor, J.M., Jansen, J.D., Olsen, L., Caffee, M.W., Fink, D., Lundqvist, J., Rosqvist, G.C., Strömberg, B., Jansson, K.N., 2016. Deglaciation of Fennoscandia. Quat. Sci. Rev. 147, 91–121.
Svendsen, J.I., Gataullin, V., Mangerud, J., Polyak, L., 2004. The glacial history of the Barents and Kara Sea Region. In: Gibbard, P.L. (Ed.), Ehlers, J. Elsevier, Developments in Quaternary Sciences, pp. 369–378.
Syvitski, J.P.M., Stein, A.B., Andrews, J.T., Milliman, J.D., 2001. Icebergs and the Sea Floor of the East Greenland (Kangerlussuaq) Continental Margin. Arct. Antarct. Alp. Res. 33, 52–61.
Todd, B.J., Valentine, P.C., Longva, O., Shaw, J., 2007. Glacial landforms on German Bank, Scotian Shelf: evidence for Late Wisconsinan ice-sheet dynamics and implications for the formation of De Geer moraines. Boreas 36, 148–169.
van der Veen, C.J., 1998. Fracture mechanics approach to penetration of bottom crevasses on glaciers. Cold Reg. Sci. Technol. 27, 213–223.
van der Vegt, P., Janszen, A., Moscariello, A., 2012. Tunnel valleys: current knowledge and future perspectives. In: Huuse, M., Redfern, J., Le Heron, D.P., Dixon, R.J., Moscariello, A., Craig, J. (Eds.), Glaciogenic Reservoirs and Hydrocarbon Systems. Geological Society, London pp, pp. 75–97.
Vorren, T.O., Laberg, J.S., 1997. Trough mouth fans - palaeoclimate and ice-sheet

monitors. Quat. Sci. Rev. 16, 865–881.
Vorren, T.O., Hald, M., Lebesbye, E., 1988. Late Cenozoic environments in the Barents Sea. Palaeoceanography 3, 601–612.
Weertman, J., 1974. Stability of the junction between an ice sheet and an ice shelf. J. Glaciol. 13, 3–11.
Wingham, D.J., Wallis, D.W., Shepherd, A., 2009. Spatial and temporal evolution of Pine Island Glacier thinning, 1995–2006. Geophys. Res. Lett. 36, L17501.
Winsborrow, M.C.M., Andreassen, K., Corner, G.D., Laberg, J.S., 2010. Deglaciation of a marine-based ice sheet: Late Weichselian palaeo-ice dynamics and retreat in the southern Barents Sea reconstructed from onshore and offshore glacial geomorphology. Quat. Sci. Rev. 29, 424–442.
Winsborrow, M.C.M., Stokes, C.R., Andreassen, K., 2011. Ice-stream flow switching during deglaciation of the southwestern Barents Sea. Geol. Soc. Am. Bull. 124, 275–290.
Wohlfarth, B., Lemdahl, G., Olsson, S., Persson, T., Snowball, I., Ising, J., Jones, V., 1995. Early Holocene environment on Bjørnøya (Svalbard) inferred from mulitdisciplinary lake sediment studies 14, 253–275. Polar Res. 14, 253–275.
Zeeberg, J.J., Lubinski, D.J., Forman, S.L., 2001. Holocene relative sea-level history of Novaya Zemlya, Russia and implications for Late Weichselian ice sheet loading. Quat. Res. 56, 218–230.